Low Complexity Dimensioning of Sustainable Solar-enabled Systems: A Case of Base Station

Suraj Suman and Swades De

Abstract—Solar-enabled systems are becoming popular for provisioning pollution-free and cost-effective energy solution. Dimensioning of a solar-enabled system requires estimation of appropriate size of photovoltaic (PV) panel as well as storage capacity while satisfying a given energy outage constraint. Dimensioning has strong impact on the user's quality of experience and network operator's interest in terms of energy outage and revenue. In this paper, dimensioning problem of solar-enabled communication nodes is analyzed in order to reduce the computation overhead, where stand-alone solar-enabled base station (SS-BS) is considered as a case study. For this purpose, hourly solar data of last ten years has been taken into consideration for analysis. First, the power consumption model of BS is revised to save energy and increase revenue. Using the hourly solar data and power consumption profile, the lower bounds on panel size and storage capacity are obtained using Gaussian mixture model, which provides a reduced search space for cost-optimal system dimensioning. Then, the cost function and energy outage probability are modeled as functions of panel size and number of battery units using curve fitting technique. The cost function is proven to be quasiconvex, whereas energy outage probability is proven to be convex function of panel size and number of battery units. These properties transform the cost-optimal dimensioning problem into a convex optimization framework, which ensures a global optimal solution. Finally, a *Computationally-efficient Energy outage aware Cost-optimal Dimensioning Algorithm (CECoDA)* is proposed to estimate the system dimension without requiring exhaustive search. The proposed framework is tested and validated on solar data of several cities; for illustration purpose, four cities, New Delhi, Itanagar, Las Vegas, and Kansas, located at diverse geographical regions, are considered. It is demonstrated that, the presented optimization framework determines the system dimension accurately, while reducing the computational overhead up to 94% and the associated energy requirement for computation with respect to the exhaustive search method used in the existing approaches. The proposed framework CECoDA takes advantage of the location-dependent unique solar profile, thereby achieving cost-efficient solar-enabled system design in significantly less time time.

Index Terms—Sustainable solar-enabled system, solar energy harvesting, cost-optimal system dimensioning, energy outage, Gaussian mixture model, curve fitting, convex optimization, computation efficiency

1 Introduction

Renewable sources of energy, such as solar and wind, are considered to be promising alternatives for powering the wireless nodes for sensing, communication, and processing activities in sensor networks [1], agricultural systems [2], home appliances [3], cellular base stations (BSs) [4], and data centers [5]. Environmentally friendly, cost-effective, and less maintenance requirement are some key features, which encourage to adopt the renewable energy based solution. Easy sunlight availability at most of the places, less costly, and noiseless operation are some important attributes, which suggest preference of solar over wind energy. Solar energy is beneficial in reducing greenhouse gas emission associated with electricity generation and achieving energy security.

A solar-enabled system requires a suitably-sized solar-energy harvesting panel and an appropriate energy storage capacity for its uninterrupted operation in absence of sufficient harvested energy. These two dimensioning requirements are interdependent. An optimal dimensioning should ensure a minimum energy outage and system cost while dealing with load profile that could be of stochastic nature. The energy harvesting and storage dimensioning principles are broadly the same for various applications, such as in wireless access infrastructure and sensor networks. In this work, we focus on stand-alone solar-enabled BSs (SS-BSs), where energy requirement profile for BS is highly time-varying due to the nature of communication traffic that the BS has to serve over 24 hours of a day.

Motivation behind our consideration of SS-BS dimensioning lies in its complexity and more generalized system configuration in terms of very long-term operation (typically, 10-15 years), replacement cost of system components (e.g., battery), and real-time traffic handling while satisfying stringent quality of service (QoS) requirements. Therefore, the analysis of cost-optimal SS-BS dimensioning covers the dimensioning related analysis of other solar-enabled systems, such as, water-pumping system, home energy, data center, sensor network, etc. Furthermore, there are a large number of geographical pockets especially in the developing countries, where the cellular BSs are not connected to power grid. In such cases, a typical BS consumes about 1500 liters of diesel per month [6]. Hence, cost-optimal energy system design of SS-BS is expected to have a high impact in realization of green communications.

The energy consumption in information and communications technology infrastructure provisioning is becoming a severe issue in terms of economy as well as environment. To address these issues, SS-BS has been gaining significant interest and is being deployed worldwide to mitigate this issue. While dimensioning the SS-BS, it requires to process very large volume of solar data for accurate dimensioning of the system, which leads to very high computation overhead and hence energy consumption. Therefore,

- *The authors are with the Department of Electrical Engineering and Bharti School of Telecommunication, Indian Institute of Technology Delhi, New Delhi 110016, India.*

design of algorithms for optimally reducing the computation overhead in SS-BS dimensioning is of great importance.

2 Background and Motivation

SS-BSs are equipped with photovoltaic (PV) panel and storage device, i.e., rechargeable battery. As the energy is harvested during the day-time only, the excess energy is required to be stored in the battery for night-time operation when no energy harvesting takes place. In SS-BSs, it is important to accurately dimension the required panel size and the number of battery units for sustainable operation in the long run while minimizing energy outage. Energy outage refers to an event when the energy required by the load exceeds the available energy in the system, and as a result routine activities of the wireless node are interrupted. Dimensioning has significant importance in terms of QoS as well as quality-of-experience (QoE) of the users' perspective - that seek minimum energy blackout, and economics from network operator's perspective - that wishes to have minimum investment and recurring costs to achieve revenue. The investment in the given context comprises capital expenditure (CapEx), operational expenditure (OpEx), and implementation expenditure (ImpEx). CapEx accounts for initial investment, OpEx accounts for the cost of replacement of system components, whereas ImpEx accounts for the rental cost. Rental cost refers to the rent of SS-BS deployment site, where cell tower, control room, and array of solar panels are being installed [7]. The solar panels cover significant space, for example, a reference solar panel of size 1 KW covers approximately 5 m^2 area. Hence, the space requirement depends upon the dimension of solar panel, because cell tower and control room have fixed dimension. This factor is important, because SS-BS is deployed for long run operation. It requires replacement of some life-limited components due to long period of operation, e.g., battery units. Over-dimensioning leads to unnecessary increased investment, whereas under-dimensioning leads to frequent energy outage.

2.1 State-of-the-Art

In cellular systems, user traffic variation is highly random. Therefore, BS dimensioning requires to capture the randomness of harvested energy as well as traffic-dependent energy consumption. Random nature of energy generation by PV panel and dynamic energy flow behavior due to day-night cycle pose major problem while dimensioning the system. Dimensioning studies can be classified into two major categories: numerical methods [6], [8], [9], [10], [11], [12], [13], [14], [15], [16] and analytical methods [17], [18], [19], [20]. Numerical methods are based on system simulation; and they offer better accuracy but involve extensive computation. In [6], the month with minimum energy generation is considered as a critical parameter, which leads to over-dimensioning. In [8], [9], [10], [11], the CapEx is minimized for a given loss of power supply probability but OpEx is not taken into consideration, whereas constant OpEx is considered in [12]. Markov chain based models are presented for estimation of energy outage in [13], [14], [15], [16]. Daily solar irradiance data is used for constructing Markov chain in [13], [14], which leads to inaccurate dimensioning. Also, these works do not consider OpEx while dimensioning. Hourly solar irradiance data is suggested as a reasonable choice for dimensioning in [21]. The energy harvested, load, and battery levels are modeled using discrete-time Markov chain with hourly solar data profile in [15]. Markov chain based model for energy outage and energy excess probability estimation is presented in [16], where the excess energy that can not be stored is sold to the power grid to earn revenue. CapEx and OpEx both are taken into consideration for obtaining the cost-optimal system dimension in [15], [16]. *Days of autonomy* criteria, defined as the consecutive number of days over which the energy generated is less than a predefined threshold, is used for dimensioning the storage capacity for a given panel size in [22], [23]. This is not a cost-optimal system; instead it leads to over-dimensioning.

Markov model [24] and Artificial Intelligence [25] based methods are also used to generate solar radiance data for places having no dataset or where large dataset is unavailable. In analytical methods, the random solar data and load data are assumed to follow some well-known distributions, such as Beta distribution [17], exponential distribution [26], and Poisson distribution [27]. Regression based techniques are also reported for dimensioning in [18], [19], [20]. The study in [18] did not consider the battery dynamics, which is a strong assumption, because battery dynamics influences the system performance. The authors in [19], [20] did not consider the randomness of data, which may lead to inaccurate dimensioning. Moreover, the cost-optimality aspect is not discussed in these studies.

To sum up, although a few methods have been reported in the literature on dimensioning of SS-BS, the procedure of estimation of cost-optimal system dimension and the corresponding computational overhead have not been investigated yet. To this end, we also note that the daily solar data used for dimensioning incurs less computation but its accuracy is questionable, whereas hourly data provides better accuracy, but the computational cost incurred is very high.

2.2 Motivation and Contributions

As discussed above, SS-BS dimensioning approaches were studied [13], [15], [16], however the considered power model for SS-BS has been the same as that for the BSs with hybrid power supply. We argue that, there is a scope of energy as well as revenue saving in SS-BS system dimensioning, because AC-to-DC conversion is not required in SS-BS system. Moreover till now, cost-optimal system dimension is estimated via the following formulation,

$$\begin{aligned} \underset{\text{(System Dimension)}}{\text{minimize}} \quad & \text{COST} \\ \text{s. t.:} \quad & \text{OUTAGE} \leq \text{outage threshold.} \end{aligned}$$

Energy outage probability for given system parameters, i.e., panel size and battery, was studied in [13], [14], [15], [16], but the methodology to select cost-optimal system dimension has not been discussed. In the existing practice, exhaustive search is used to estimate the optimal system dimension while satisfying a given energy outage constraint, which is computationally extensive. The existing deployments only consider CapEx optimal system [13], [14]. In contrast, for SS-BS, jointly CapEx, OpEx, and ImpEx optimal system is preferred [15], [16]. However, as compared to only CapEx-optimal dimensioning, computation issue is more severe in case of CapEx, OpEx, and ImpEx optimal dimensioning. The tradeoff for system dimensioning process lies in the accuracy, volume of data used, and computation time. For accurate dimensioning, volume of data with fine granularity is used, which involves high computational time. Accuracy of dimensioning has significant importance in terms of energy outage performance and revenue, whereas the computational overhead translates to processing-related energy consumption. Therefore, a

computationally-efficient framework on optimal dimensioning of the SS-BS is of practical interest.

Key contributions of this work are as follows:

- A power consumption model is presented for SS-BS that relies only on solar energy; the model aids in achieving cost-effective green communication system design. The cost saving up to 12% has been observed by using this model.
- Lower bounds on system dimension, namely, panel size and the number of batteries, are obtained using Gaussian mixture model (GMM).
- By curve fitting technique, battery life is modeled as a function of panel size and number of batteries. The total cost, comprising of CapEx, OpEx, and ImpEx, is proved to be quasiconvex, whereas the energy outage is proved to be a convex function of system dimension. Accordingly, the cost-optimal dimensioning problem is transformed into a convex optimization framework, where the objective function (total cost) is quasiconvex and the constraints (energy outage and lower bound on system dimension) are convex. Convexity ensures the global optimal solution.
- A *Computationally-efficient Energy outage aware Cost-optimal Dimensioning Algorithm (CECoDA)* is presented for system dimensioning for a given energy outage constraint. CECoDA is initialized with obtained lower bound.
- We have investigated the performance of proposed analytical framework with data from several cities of India (New Delhi, Itanagar, Ahmedabad, Kolkata, Jaipur, Mumbai, Hyderabad) and USA (Las Vegas, Kansas, Denver, Texas, Missouri, Illinois, Indiana, New York) situated at diverse geographical locations with different traffic profiles. For brevity of presentation, four cities New Delhi, Itanagar, Las Vegas, and Kansas are considered for illustrative numerical performance results. A comparative study of dimensioning performance of the proposed optimization framework with respect to the exhaustive search method, which is used in existing practice, demonstrates significant reduction in computation overhead with accurate system dimension estimation. Reduction in computation time up to 94% has been noticed.

2.3 Scope and Significance

Reduction in computation time is very crucial issue, not only for speeding up the system performance, but also to reduce the energy consumption. As noted in [28], computation of 1 bit data requires approximately 0.1 μJoule of energy. For an SS-BS deployed at a given location, even with the same solar radiation profile, any change in system parameters, such as, energy outage constraint, cost of solar panel, cost and capacity of battery, traffic profile, site rent, etc., exhaustive search process needs to be repeated, which is expensive. Moreover, solar irradiance, user traffic profile, and other system parameters could be location-specific, hence site-specific computation overhead has to be incurred, which is expected to further increase with proliferation of cellular coverage using small cells and large-scale solar-enabled monitoring applications. Therefore, light-weight solar-enabled system dimensioning is expected to have a wide interest.

Although only SS-BS has been discussed here due to lack of space, the analysis presented can be applied to characterize other solar-enabled systems, such as, home appliances, agricultural systems, and sensor networks.

2.4 Paper Organization

The paper is organized as follows. Section 3 presents a new power consumption model for SS-BS and lower bounds on system dimension. The cost function is modeled in Section 4, and the energy outage probability is analyzed in Section 5. The proposed CECoDA is presented in Section 6, followed by the results and discussion in Section 7. The paper is concluded in Section 8.

Table 1: List of important variables along with their descriptions

n_{PV}	Size of PV panel
N_B	Number of battery
e_H^{1KW}	Energy harvested by PV panel size of 1 KW
$e_H^{n_{PV}}$	Energy harvested by PV panel size of n_{PV}
n_c	Charging efficiency of battery
n_d	Discharging efficiency of battery
$n_{PV_{LB}}$	Lowe bound of PV panel
$N_{B_{LB}}$	Lower bound on number of battery
C_{CapEx}	Capital expenditure
C_{OpEx}	Operational expenditure
C_{ImpEx}	Implementation expenditure
C_{Ex}	Total expenditure
C_{PV}	Cost of reference PV panel size of 1 KW
C_B	Cost of a battery
A_{PV}	Area of reference PV panel size of 1 KW
Y	Duration of operation of BS
C_R	Rental cost of unit area land
DoD	Depth-of-discharge of battery
P_{out}	Energy outage probability
L	Lifetime of battery

3 Evaluation of Lower Bound on System Dimension

SS-BS system model shown in Fig. 1 consists of PV panels as energy harvester, a set of battery as energy storage device, and BS as energy consumer or load. Energy can be extracted from battery whenever the harvested energy by the PV panel is less than the required consumption. If instead, the energy harvested is more than the required consumption, energy is added to the battery. Solar energy profile and power consumption profile of BS are required to be analyzed for cost-effective system dimensioning.

Solar radiation data provides information on how much of the Sun's energy strikes the solar panel surface during a particular time period. For this purpose, statistical solar data of last 10 years has been accessed from National Renewable Energy Laboratory (NREL). This large volume of data over such a long period also incorporates the seasonal variations. This data is fed into the System Advisor Model (SAM) to get the hourly energy generated by a panel of 1 KW rating i.e., e_H^{1KW} with default settings [29]. SAM is a performance modeling software designed for renewable energy industry. For analysis and illustration, a few geographically diverse locations having different solar energy generation capabilities are considered. Here, two cities from India (New Delhi and Itanagar) and two cities from USA (Las Vegas and Kansas). Itanagar is a hilly area that exhibits significant hourly irradiance variation, whereas New Delhi is a plain land area. Las Vegas has more sunny days than Kansas, whereas Kansas has more rainy days than Las Vegas.

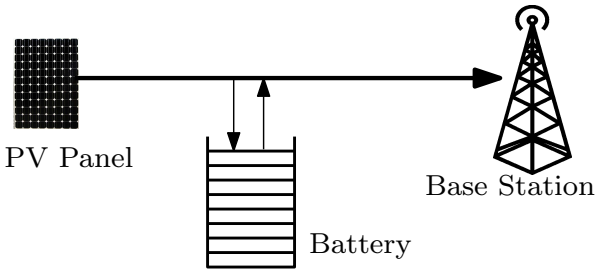

Figure 1: System model for stand-alone solar-enabled base station (SS-BS).

Table 2: Power consumption of different components and nature of their operating voltage for Macro BS

Component name	Power consumption	Operating voltage
Power amplifier	128.2 W	DC
RF transceiver	13.5 W	DC
Baseband	29.5 W	DC
DC-DC	13.5	DC
Cooling	22.5 W	DC, AC both
Main supply	18 W	AC

Table 3: The parameters of power model for SS-BS

BS type	N_{trx}	P_{max} (W)	$P_o^{\text{SS-BS}}$ (W)	Δ
Macro	6	20	112	4.7
Micro	2	6.3	50	2.6
Pico	2	0.13	6	4
Femto	2	0.05	4.25	8

3.1 Proposed Power Consumption Model of SS-BS

The basic power consumption model for BS is given by [30]:

$$P^{BS}(t) = N_{trx} \cdot (P_o + \Delta \cdot \rho(t) \cdot P_{max}), \tag{1}$$

where N_{trx} is the number of transceiver, P_o is the power consumption at zero RF output power, Δ is the slope of load dependent power consumption, P_{max} is the maximum RF output power at maximum load, and $0 \leq \rho(t) \leq 1$ is the normalized traffic at time t. The values of these parameters are different for different type of BSs. For macro BS, which is considered for analysis in this work, $N_{trx} = 6, P_o = 130$ W, $\Delta = 4.7$, $P_{max} = 20$ W, and the hourly normalized traffic profile $\rho(t)$ is shown in Fig. 2. The traffic profile considered has been generated from the data collected from LTE macro BS of Vodafone mobile operator with coverage radius of 500 m [21].

The model given in (1) comprises power consumption by several components, namely power amplifier, radio frequency (RF) transceiver, baseband, DC-DC, cooling, and AC-DC (main supply). Power consumed by each component and the nature of their operating voltage are listed in Table 2 for a typical macro BS [31], [32]. It may be noted that, main supply contributes approximately 8 % (18 W), which primarily due to AC to DC power conversion. Then DC-DC converter supplies the required DC voltage to the other components, i.e., power amplifier, RF transceiver, baseband. The cooling system can operate on AC as well as DC supply. Table 2 indicates that the DC power supply is sufficient to operate the SS-BSs, as they are not connected to grid; PV panels generate the required DC power. Therefore, by removing the main supply unit and operating only by the DC power generated from the PV panel can save significant amount of energy in normal as well as sleep mode of operation. This mechanism can also save significant amount of energy in other types of SS-BSs, such as micro, pico and femto BS, where the main supply consumes approximately 8 %, 11%, and 11 %, respectively [33]. Considering the above modification by removing the main supply unit, the new power consumption model for SS-BS suggested here is given as,

$$P^{\text{SS-BS}}(t) = N_{trx} \cdot (P_o^{\text{SS-BS}} + \Delta \cdot \rho(t) \cdot P_{max}). \tag{2}$$

Parameters of the new power consumption model are listed in Table 3.

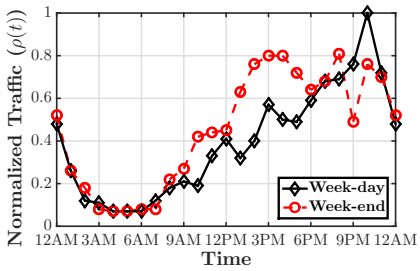

Figure 2: Variation of hourly traffic profile during weekdays and weekends.

3.2 Evaluation of Lower Bound on System Dimension

Using the hourly solar data and power consumption profile (cf. (2)), the lower bound on system dimension (PV panel and storage) is estimated. Let the charging and discharging efficiency of the lead acid battery be denoted by η_c and η_d, respectively. Assume that the system has sufficient storage, such that the energy is available in the battery whenever required. This is a valid assumption while evaluating the lower bounds. Let e_{cons} denotes the hourly energy consumption by BS obtained from (cf. (2)) using the hourly traffic profile shown in Fig. 2.

3.2.1 *Modeling of Leftover Energy*

Energy harvested by the PV panel of size n_{PV} (i.e., having n_{PV} units of solar cells in the panel) is given as,

$$e_H^{n_{PV}}(t) = n_{PV} \cdot e_H^{1KW}(t), \tag{3}$$

where t denotes the hour index, as hourly data is available.

The battery energy dynamics, which involves charging-discharging phenomena, is given by,

$$B(t) = B(t-1) + e_{\mathcal{L}}^{n_{PV}}(t), \tag{4}$$

where $e_{\mathcal{L}}^{n_{PV}}(t)$ is the leftover energy at time instant t and given by,

$$e_{\mathcal{L}}^{n_{PV}}(t) = \begin{cases} \eta_c\big(e_H^{n_{PV}}(t) - e_{cons}(t)\big), & e_H^{n_{PV}}(t) \geq e_{cons}(t) \\ \frac{1}{\eta_d}\big(e_H^{n_{PV}}(t) - e_{cons}(t)\big), & e_H^{n_{PV}}(t) < e_{cons}(t) \end{cases}. \tag{5}$$

Positive leftover energy indicates that, the harvested energy is greater than energy usage by the load, and the excess energy is added to the battery. Negative leftover energy indicates that, the harvested energy is less than the energy demand by the load, and the required energy is withdrawn from the battery.

Empirically obtained probability distribution function (PDF) of leftover energy at a SS-BS in Las Vegas city is shown in Fig. 3(a). The variation of pdf of leftover energy does not follow any standard distribution; it has several peaks. Therefore, we model

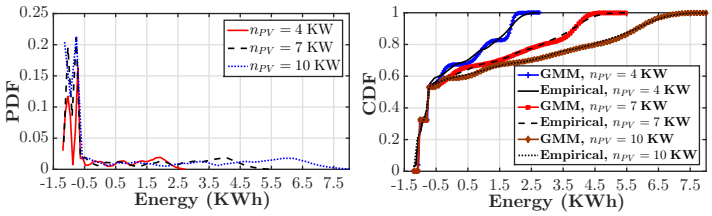

(a) empirical pdf (b) cdf of empirical and GMM

Figure 3: (a) Empirical pdf, and (b) cdf obtained empirically and by GMM for Las Vegas city, with n_{PV} = 5 KW, 8KW, and 11 KW; $\eta_c = 0.9$, $\eta_d = 0.9$.

it by Gaussian mixture model (GMM). GMM is a probabilistic model that assumes all the data points are generated from a mixture of a finite number of Gaussian distributions. Each Gaussian component is associated with a normalized weight, which indicates its proportion in the distribution [34]. The hourly data for all the years solar energy generation is considered to parameterize the leftover energy. Large volume of dataset offers better fitting accuracy; it also incorporates the seasonal variations.

Let $E_{\mathcal{L}}^{n_{PV}}$ denote the random variable that captures the variation of hourly leftover energy $e_{\mathcal{L}}^{n_{PV}}$ for a given n_{PV}. The GMM modeled distribution of $E_{\mathcal{L}}^{n_{PV}}$ in (5), i.e., the distribution of the random variable $E_{\mathcal{L}}^{n_{PV}}$, is expressed as:

$$f_{E_{\mathcal{L}}^{n_{PV}}}(e) = \sum_{i=1}^{K} \frac{\alpha_i^{n_{PV}}}{\sqrt{2\pi}\cdot\sigma_i^{n_{PV}}} \cdot \exp\Big(\frac{-(e-\mu_i^{n_{PV}})^2}{2\cdot(\sigma_i^{n_{PV}})^2}\Big), \quad (6)$$

where K is the number of Gaussian components used to model the data. $\alpha_i^{n_{PV}}$, $\mu_i^{n_{PV}}$, and $\sigma_i^{n_{PV}}$ are respectively weight, mean, and standard deviation of the i^{th} Gaussian component for a given panel size n_{PV}. The weights of all components in GMM satisfies $\sum_{i=1}^{K} \alpha_i^{n_{PV}} = 1$.

In Fig. 3(a), the negative index of $E_{\mathcal{L}}^{n_{PV}}$ denotes the energy extracted from the storage, whereas positive index denotes the energy added to the storage. Kolmogorov-Smirnov (KS) test is used to identify the suitable number of Gaussian components (K) for fitting [35]. KS distance is the maximum distance between empirical cumulative distribution function (CDF) and estimated CDF using GMM. When the change in KS distance between two successive GM models is below a threshold, then addition of number of components is stopped. The CDF of empirical data and GMM are shown in Fig. 3(b) for different panel size at a SS-BS in Las Vegas city. For a given KS distance threshold 0.05, the best GMM fit for the four cities, New Delhi, Itanagar, Las Vegas, and Kansas, with $n_{PV} = 5$ KW are achieved with $K = 5$, 7, 6, and 6, respectively.

3.2.2 Lower Bound on System Dimension

Using the developed GMM distribution of leftover energy in (6), the mean of hourly leftover energy is obtained as,

$$\mathbb{E}\Big[E_{\mathcal{L}}^{n_{PV}}\Big] = \int_{-\infty}^{\infty} e \cdot f_{E_{\mathcal{L}}^{n_{PV}}}(e)\cdot de = \sum_{i=1}^{K} \alpha_i^{n_{PV}} \cdot \mu_i^{n_{PV}}. \quad (7)$$

For a sustainable system in the long run, the mean of hourly leftover energy should be positive to avoid the energy outage in each hour on an average. This indirectly indicates the energy neutrality on hourly basis, and overall, the energy is added to storage in each hour. If instead the mean leftover energy is negative, then on average the energy is extracted from storage in each hour, thereby leading to depletion of stored energy and subsequent energy outage.

Thus, for a green sustainable system in long run, $\mathbb{E}\Big[E_{\mathcal{L}}^{n_{PV}}\Big] \geq 0$. Accordingly, the lower bound on PV panel size $n_{PV_{LB}}$ is expressed as:

$$n_{PV_{LB}} = \inf\Big\{n_{PV} | \sum_{i=1}^{K} \alpha_i^{n_{PV}} \cdot \mu_i^{n_{PV}} \geq 0\Big\}, \quad (8)$$

where `inf` indicates the infimum.

The mean energy extracted from storage in each hour $S_h^{n_{PV}}$ for a given panel size n_{PV} corresponds to the negative index of leftover energy profile and is expressed as:

$$\begin{aligned} S_h^{n_{PV}} &= \int_{-\infty}^{0} e \cdot f_{E_{\mathcal{L}}^{n_{PV}}}(e)\cdot de \\ &= \int_{-\infty}^{0} e \cdot \sum_{i=1}^{K} \frac{\alpha_i^{n_{PV}}}{\sqrt{2\pi}\cdot\sigma_i^{n_{PV}}} \cdot \exp\Big(\frac{-(e-\mu_i^{n_{PV}})^2}{2(\sigma_i^{n_{PV}})^2}\Big)\cdot de, \\ &= \sum_{i=1}^{K} \frac{\alpha_i^{n_{PV}}}{\sqrt{2\pi}} \cdot \Big[\sqrt{2\pi}\cdot\mu_i^{n_{PV}} \cdot \Big(1 - Q(\frac{-\mu_i^{n_{PV}}}{\sigma_i^{n_{PV}}})\Big) - \\ &\qquad \sigma_i^{n_{PV}} \cdot \exp\Big(\frac{-(\mu_i^{n_{PV}})^2}{2(\sigma_i^{n_{PV}})^2}\Big)\Big], \end{aligned} \quad (9)$$

where $Q(\cdot)$ denotes the Q-function.

Typically, solar radiation is available during day hours only. The 24 hours period constitutes a cycle over which charging and discharging occurs. On average, the total energy extracted in each cycle is $S_d^{n_{PV}} = 24.S_h^{n_{PV}}$.

Therefore, for a panel size n_{pV}, the storage capacity required $S^{n_{PV}}$ is governed by,

$$\begin{aligned} S^{n_{PV}} &\geq |S_d^{n_{PV}}| \\ &= 24 \cdot \Big| \sum_{i=1}^{K} \frac{\alpha_i^{n_{PV}}}{\sqrt{2\pi}} \cdot \Big[\sigma_i^{n_{PV}} \cdot \exp\Big(\frac{-(\mu_i^{n_{PV}})^2}{2(\sigma_i^{n_{PV}})^2}\Big) - \\ &\qquad \sqrt{2\pi}\cdot\mu_i^{n_{PV}} \cdot \Big(1 - Q(\frac{-\mu_i^{n_{PV}}}{\sigma_i^{n_{PV}}})\Big)\Big]\Big| = S_{LB}^{n_{PV}}. \end{aligned} \quad (10)$$

where $S_{LB}^{n_{PV}}$ is the lower bound on storage. It indicates that, at least this amount of energy should be available, such that whenever harvested energy is less than the required consumption, the storage is able to supply. $S_{LB}^{n_{PV}}$ also depends on the panel size. Thus, the lower bound on number of battery units can be obtained as,

$$N_{B_{LB}} = \Big\lceil \frac{S_{LB}^{n_{PV}}}{\delta \cdot B_{cap}} \Big\rceil. \quad (11)$$

where B_{cap} is the capacity of each battery and δ is the depth-of-discharge of each battery.

Remark 1. *For very large panel size, the storage required during radiation hours reduces to very small or insignificant value, whereas storage requirement remains vital during absence of radiation. Let us denote energy storage requirement in absence of radiation by $N_{B_{th}}$; it can be obtained as,*

$$S_{th} = \lim_{n_{PV}\to\infty} S_{LB}^{n_{PV}} \Rightarrow N_{B_{th}} = \Big\lceil \frac{S_{th}}{\delta.B_{cap}} \Big\rceil. \quad (12)$$

It is notable that, unlike $N_{B_{LB}}$, $N_{B_{th}}$ is independent of panel size with $N_{B_{LB}} \geq N_{B_{th}}$, and due to its independency from n_{PV},

it is used in the formulation of optimization problem in subsequent sections.

4 Modeling of Cost Function

In green sustainable system, it is important to choose the number of PV panels and battery units in cost-optimal sense, such that the long-run energy outage remains within an acceptable range. The expenditure in the given context refers to the cost of PV panel and battery, which comprises of mainly three parts: CapEx, OpEx, and ImpEx. Other costs, such as, components, manpower, and transportation are supposed to be constant and have no impact on system dimensioning.

4.1 CapEx

CapEx accounts for the initial investment, which includes the dimensioning-related costs, namely, the cost of PV panel, battery, and equipment. Accordingly, CapEx of SS-BS is captured as:

$$C_{CapEx}(n_{PV}, N_B) = C_{PV} \cdot n_{PV} + C_B \cdot N_B + C_0, \quad (13)$$

where C_{PV} and C_B denote the cost of reference panel of size 1 KW and cost of a battery unit, respectively. C_0 captures the constant costs.

C_0 includes the cost of BS components, such as digital signal processor, power amplifier, transceiver, antenna, cellular tower, etc. The cost of these components do not depend on n_{PV} and N_B. Also, they have sufficiently long lifetime and hence these are deployed once, unlike the battery units which have limited lifetime. Thus, C_0 is not influenced by the system dimension and is treated as constant in the given context. Therefore, for compactness the actual cost of these components are not considered in the optimization framework.

4.2 OpEx

Usually, SS-BSs are installed for long period of operation, i.e., for 10 to 20 years. Hence, it involves replacement of life-limited components, i.e., battery in the current context. OpEx accounts for this cost, which is explored as:

$$C_{OpEx}(n_{PV}, N_B) = C_B \cdot N_B \cdot \frac{Y}{L(n_{PV}, N_B)} - C_B \cdot N_B + C_1, \quad (14)$$

where Y denotes the period of operation in years and $L(n_{PV}, N_B)$ denotes the lifetime of battery with system dimension (n_{PV}, N_B). C_1 is a constant, which includes other costs. $C_B \cdot N_B$ term is deducted from OpEx, because it is included in CapEx at the time of installation.

Battery life is an important factor in renewable energy based systems, because it has a strong impact on OpEx. In general, lifetime depends on the number of cycles and depth-of-discharge (*DoD*) in each cycle. *DoD* indicates the percentage of charge extracted from the battery. A lower *DoD* per cycle offers a higher lifetime, and vice-versa. Due to random nature of energy harvested and absence of solar irradiance during night hours, the *DoD* varies significantly over each cycle, which causes degradation of battery life. Rainflow counting algorithm [36] is a widely used technique to count the total number of cycles for a given battery energy dynamics. The number of cycles against *DoD* data given in the data-sheet of battery [37] is used here to obtain the lifetime of a set of battery units. Using curve fitting technique, the number of cycles against the *DoD* is found to vary as:

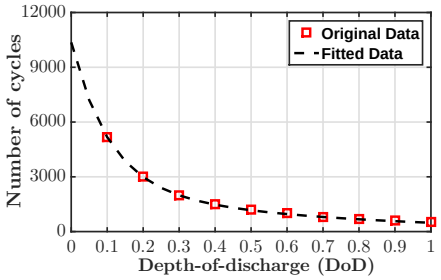

Figure 4: Variation of number of cycles against depth-of-discharge (*DoD*).

$$N_c(DoD) = 7855 \cdot \exp(-9.48 \cdot DoD) + 2508 \cdot \exp(-1.605 \cdot DoD). \quad (15)$$

The variation of fitted and original number of cycles against the *DoD* is shown in Fig. 4, which depicts excellent fitting with R-squared value 0.9994.

The temperature dependence of number of cycles is captured as:

$$N_c(DoD, T) = N_c(DoD) \cdot \left(37.68 \cdot T^{-1.101} - 0.3897\right), \quad (16)$$

where T denotes the temperature in °C. Here, $T = 27$°C is considered, where full battery capacity is available [37] and this temperature can be maintained using cooling system.

The battery life for a given system dimension (n_{PV}, N_B) is evaluated as,

$$L(n_{PV}, N_B) = \frac{1}{\sum_{k=1}^{\mathcal{N}_C} \frac{1}{N_c(DoD_k, T=27°\text{C})}}, \quad (17)$$

where $\mathcal{N}_C$ is the total number of cycles obtained from Rainflow counting algorithm [36] and $N_c(DoD_k)$ is the number of cycles corresponding to DoD of k^{th} cycle. Battery life depends on the panel size as well as the number of battery units, because the energy harvested by panel dictates the *DoD* of battery.

4.3 ImpEx

ImpEx accounts for the cost to rent a site, construction, and installation. The rental cost depends on the area of site required to set up the BS as well as to install PV panel. Thus, the ImpEx of SS-BS is expressed as,

$$C_{ImpEx}(n_{PV}, N_B) = A_{PV} \cdot n_{PV} \cdot Y \cdot C_R + C_2, \quad (18)$$

where A_{PV} denotes the area covered by a reference panel of size 1 KW rating, C_R denotes the rent per unit area per year, Y denotes the number of years for operation. C_2 is a constant, which includes the other costs, namely, construction and installation costs. The area covered by BS set up is incorporated in constant part and only PV panel size dependent rent is taken into consideration.

4.4 Characterization of Cost Function

The total expenditure, i.e., cost function is given as,

$$\begin{aligned} C_{Ex}(n_{PV}, N_B) &= C_{CapEx}(n_{PV}, N_B) + C_{OpEx}(n_{PV}, N_B) + \\ &\quad C_{ImpEx}(n_{PV}, N_B) \\ &= C_{PV} \cdot n_{PV} + C_B \cdot \frac{Y}{L(n_{PV}, N_B)} \cdot N_B + \\ &\quad C_R \cdot n_{PV} \cdot A_{PV} \cdot Y + C_{all}, \end{aligned} \tag{19}$$

where $C_{all} = C_0 + C_1 + C_2$ accounts for all constants.

The cost function depends upon n_{PV}, N_B, and $L(n_{PV}, N_B)$. The expression of battery life in (17) is not analytically tractable, because it depends upon the depth-of-discharge of each cycle and the number of cycles. Both of these quantities have no closed form expression as function of n_{PV} and N_B, because the depth-of-discharge as well as number of cycle is dictated by the battery dynamics. Therefore, the battery life for each system combination (n_{PV}, N_B) is calculated, and its nature is explored using an empirical equation obtained from curve fitting technique [38]. In order to examine the accuracy of fitting, two goodness-of-fit parameters R-square and root mean square error (RMSE) have been used.

Battery life for different system dimension (n_{PV}, N_B), where each battery has capacity rating 12 V, 205 Ah with $\delta = 0.7$, is obtained and fitted using curve fitting technique. The following empirical equation captures the battery life as function of n_{PV} and N_B,

$$\begin{aligned} L(n_{PV}, N_B) &= a_{00} + a_{10} \cdot n_{PV} + a_{01} \cdot N_B + a_{11} \cdot n_{PV} \cdot N_B \\ &\quad + a_{20} \cdot {n_{PV}}^2 + a_{02} \cdot N_B^2 + a_{21} \cdot {n_{PV}}^2 \cdot N_B + \\ &\quad a_{12} \cdot n_{PV} \cdot N_B^2 + a_{30} \cdot {n_{PV}}^3 + a_{03} \cdot N_B^3. \end{aligned} \tag{20}$$

The fitting coefficients a_{ij}'s for four different cities are listed in Table 4 along with the values of goodness-of-fit parameters. The R-square value close to 1 and very small RMSE value indicate the accuracy of curve fitting.

Remark 2. *We restrict our analysis for system dimension in the range: $n_{PV_{LB}} \leq n_{PV} \leq 20$ KW, $N_{B_{th}} \leq N_B \leq 75$, which is sufficient for practical deployment perspective of SS-BS. Consideration of a higher system dimension does not have practical consequence, although the presented analysis remains valid for higher system dimension as well.*

Remark 3. *The panel size n_{PV} and the number of battery units N_B are considered as continuous variables for characterization of the cost-optimal dimensioning problem. Actually, storage and panel size are continuous variables; but in practical deployment scenario, the number of battery units is integer-valued and some fixed increment in panel size, e.g., 0.5 KW or 1 KW is considered. This assumption is used only to characterize the cost-optimal dimensioning problem; it will not affect the cost-optimal solution.*

Theorem 1. *The total expenditure $C_{Ex}(n_{PV}, N_B)$ is quasiconvex function of system dimension, i.e. panel size n_{PV} and the number of battery units N_B.*

Proof: See Appendix A. □

Theorem 1 can be interpreted as follows: When the deployed number of PV cells n_{PV} and battery units N_B are small, the CapEx is less. However, this small value of n_{PV} and N_B lead to frequent discharge of the battery units due to lesser energy generation and energy storage capacity. Consequently, this causes a higher DoD in charging cycles which results in effectively less number of tolerable charging cycles of battery units, and hence its lifetime is reduced. Thus, more frequent requirement of battery replacement causes a higher OpEx. On the other hand, CapEx is very high when the deployed numbers of n_{PV} and N_B are high. However, the battery does not discharge severely, i.e., DoD is lesser due to high energy generation as well as energy storage capacity. A lesser DoD in a charging cycle in turn offers effectively a high number of charging cycles. Hence, the lifetime of a battery unit is longer, which leads to a lesser OpEx. These extreme cases exist at boundary; the cost decreases in between them, thus offering a quasiconvex nature of the total expenditure.

Table 4: Fitting coefficients and the values of goodness-of-fit parameters for battery life, for different cities

New Delhi	$a_{00} = -20.77$, $a_{10} = 5.421$, $a_{01} = -0.04516$, $a_{20} = -0.4413$, $a_{11} = 0.05719$, $a_{02} = -0.00314$, $a_{21} = -0.00148$, $a_{12} = -0.0001483$ $a_{30} = 0.01104$, $a_{03} = 2.338 \times 10^{-5}$ RMSE $= 0.5296$, R-square $= 0.9788$
Itanagar	$a_{00} = -23.25$, $a_{10} = 5.496$, $a_{01} = -0.2862$, $a_{20} = -0.4133$, $a_{11} = 0.07376$, $a_{02} = -0.001004$, $a_{21} = -0.001811$, $a_{12} = -0.0001966$ $a_{30} = 0.009762$, $a_{03} = 1.493 \times 10^{-5}$ RMSE $= 0.3221$, R-square $= 0.9919$
Las Vegas	$a_{00} = -10.47$, $a_{10} = 3.177$, $a_{01} = -0.05632$, $a_{20} = -0.2839$, $a_{11} = 0.05388$, $a_{02} = -0.002656$, $a_{21} = -0.001407$, $a_{12} = -0.0001344$, $a_{30} = 0.00751$, $a_{03} = 1.195 \times 10^{-5}$, RMSE $= 0.4316$, R-square $= 0.9847$
Kansas	$a_{00} = -4.273$, $a_{10} = 1.525$ $a_{01} = -0.1649$, $a_{20} = -0.1442$, $a_{11} = 0.0527$, $a_{02} = -0.001224$, $a_{21} = -0.001251$, $a_{12} = -0.000132$, $a_{30} = 0.00389$, $a_{03} = 1.229 \times 10^{-5}$ RMSE $= 0.1918$, R-square $= 0.9964$

5 Analysis of Energy Outage Probability

Energy outage happens when neither PV panel nor storage is able to supply the required energy. Energy availability, which is the complement of energy outage, is measured using number of 9's [39]. For example, two 9's indicate 99% availability, or 1% energy outage, which means about 15 minutes of energy blackout daily. Up to 1% energy outage is considered acceptable in cellular BS operation [4]. Maintaining a low energy outage is also important because a BS takes several minutes to start functioning after a shut-down [40]. The energy outage probability for a given panel size and the number of battery is calculated from (21) using the hourly harvested energy. Here $B(t)$ is the energy level of battery at time t, N_B is the number of battery, B_{cap} is the capacity of each battery unit, $e_H^{n_{PV}}(t)$ is the hourly energy harvested by panel of size n_{PV}, $e_{cons}(t)$ is the hourly energy consumed by BS at time t, and δ is the depth-of-discharge of battery. $I(\cdot)$ is an indicator function, given as:

$$I(x) = \begin{cases} x, & \text{if } x \geq 0 \\ 0, & \text{if } x < 0. \end{cases}$$

$$B(t) = \begin{cases} N_B \cdot B_{cap}, & \text{if } B(t) \geq N_B \cdot B_{cap} \\ B(t-1) + \eta_c \cdot I\Big(e_H^{n_{PV}}(t) - e_{cons}(t)\Big) + \frac{1}{\eta_d} \cdot I\Big(e_{cons}(t) - e_H^{n_{PV}}(t)\Big), & \text{if } (1-\delta) \cdot N_B \cdot B_{cap} < B(t) < N_B \cdot B_{cap} \\ (1-\delta) \cdot N_B \cdot B_{cap}, & \text{if } B(t) \leq (1-\delta) \cdot N_B \cdot B_{cap}. \end{cases} \quad (21)$$

Table 5: Fitting coefficients and the values of goodness-of-fit parameters for energy outage probability, for different cities

New Delhi	$b_{00} = 0.01413$, $b_{10} = 20.28$, $b_{01} = -0.0006561$, $b_{20} = 7372$, $b_{11} = -0.2659$, $b_{02} = 6.71 \times 10^{-6}$, RMSE $= 0.0043$, R-square $= 0.9434$
Itanagar	$b_{00} = 0.01413$, $b_{10} = 121.83$, $b_{01} = -0.001797$, $b_{20} = 11391$, $b_{11} = -0.1121$, $b_{02} = 1.691 \times 10^{-5}$, RMSE $= 0.00109$, R-square $= 0.9664$
Las Vegas	$b_{00} = 0.01888$, $b_{10} = 38.80$, $b_{01} = -0.0008892$, $b_{20} = 2886$ $b_{11} = -0.2997$, $b_{02} = 9.023 \times 10^{-6}$ RMSE $= 0.0047$, R-square $= 0.9667$
Kansas	$b_{00} = 0.01729$, $b_{10} = 17.21$ $b_{01} = -0.0006997$, $b_{20} = 1378$, $b_{11} = -0.1327$, $b_{02} = 6.582 \times 10^{-6}$, RMSE $= 0.0027$, R-square $= 0.9384$

Here also, highly random nature of harvested energy and battery dynamics restrict the analytical tractability of variation of outage probability as a function of system dimension, i.e. n_{PV} and N_B. Equation (21) is an iterative expression, where the batteries can be charged up to its maximum capacity and discharged up to its DoD. The operation is not allowed beyond this range.

A closed-form expression of energy outage probability as a function of n_{PV} and N_B is not available. To this end, in this work curve fitting technique is used to obtain an empirical expression for analyzing the system dimensioning further. For this purpose, energy outage probability for each system dimension is calculated, and its variation as a function of n_{PV} and N_B is obtained. Energy outage probability as a function of system dimension is captured using the following empirical equation:

$$P_{out}(n_{PV}, N_B) = b_{00} + b_{10} \cdot e^{-n_{PV}} + b_{01} \cdot N_B + b_{11} \cdot e^{-n_{PV}} \cdot N_B + b_{20} \cdot e^{-2n_{PV}} + b_{02} \cdot N_B^2. \quad (22)$$

The fitting coefficients b_{ij}'s for four different cities are listed in Table 5 along with the goodness-of-fit values. The R-square values are close to 1 and RMSE values are very small, which indicate the accuracy of the empirical expression.

It may be noted from (22) that, the energy outage probability decreases with increase in n_{PV} and N_B values, but the decay is exponential with increase of n_{PV}. Larger PV panel generates higher energy, which leads to sufficient energy availability in the battery units, and thus it reduces the outage probability.

Theorem 2. *The energy outage probability $P_{out}(n_{PV}, N_B)$ is convex function of system dimension, i.e., PV panel size n_{PV} and number of battery units N_B.*

Proof: See Appendix B. □

Theorem 2 can be interpreted as follows: For smaller n_{PV} and N_B deployment, frequent energy outage happens due to lesser energy generation and energy storage capacity. On the other hand, larger n_{PV} and N_B avoid energy outage due to higher energy generation and energy storage capacity. Also, with increase in either n_{pV} or N_B, the harvested energy or storage capacity increases, which reduces the energy outage. This indicates that, the energy outage will improve significantly with increase in system dimension, which leads to the convex nature.

6 Computationally-efficient Cost-Optimal Dimensioning

Till now, the feasible search space is identified in Section 3, and cost function and energy outage are characterized in Sections 4 and 5, respectively. In this section, the cost-optimal system dimensioning is performed using the analysis in previous sections. The optimization problem for cost-optimal dimensioning while satisfying the energy outage constraint is formulated as:

$$\begin{aligned} \text{(P1)}: \underset{(n_{PV}, N_B)}{\text{minimize}} \quad & C_{Ex}(n_{PV}, N_B) \\ \text{subject to:} \quad & P_{out}(n_{PV}, N_B) \leq p, \\ & -n_{PV} \leq -n_{PV_{LB}}, \\ & -N_B \leq -N_{B_{th}}, \end{aligned}$$

where $C_{Ex}(n_{PV}, N_B) = C_{CapEx}(n_{PV}, N_B) + C_{OpEx}(n_{PV}, N_B) + C_{ImpEx}(n_{PV}, N_B) = C_{PV} \cdot n_{PV} + C_B \cdot \frac{Y}{L(n_{PV}, N_B)} \cdot N_B + C_R \cdot n_{PV} \cdot A_{PV} \cdot Y + C_{all}$.

Theorem 1 and Theorem 2 reveal that, the objective function (total expenditure or total cost) is quasiconvex function of system dimension and the constraints (energy outage probability and lower bounds) are convex functions of system dimension. Thus, Theorem 1 and Theorem 2 transform the optimization problem (P1) into a convex optimization framework [41], which ensures a global optimal.

Remark 4. *The cost-optimal dimensioning problem while satisfying the energy outage constraint is convex. Therefore, the local optimal solution overlaps with the global optimal solution.*

The emphasis is on characterizing the optimization problem (P1) rather than solving it, because it provides the clue about the variation of function, and indicates where to stop the process. In this work, we will take the advantage of convexity of (P1) to reach the optimal solution in computationally efficient way. On the other hand, one needs the empirical equations (20) and (22) in order to solve (P1) for a given city. This requires computation of battery life (cf. (17)) and outage probability (cf. (21)) by exhaustive search, involving significant overhead. Also, the cost-optimal system dimension should be integer valued from real life deployment perspective, but (P1) does not provide integer solution. Rounding the non-integer value to integer value will lead to over-dimensioning or under-dimensioning. Thus, solving (P1) is neither computationally efficient nor serves the purpose. On the other hand, the empirical equations (20) and (22) are obtained to characterize the system behavior, which remains valid in general.

Although convexity ensures the global optimal solution, our aim is to reach this cost-optimal solution $(n_{PV}^{opt}, N_B^{opt})$ in minimum time. Therefore, we need to come up with a procedure

such that the minimum number of system combinations could be traversed while achieving an optimal solution. The path to optimal solution can be traversed in depth first search fashion due to the discrete nature of variables (n_{PV} and N_B), where the search for optimal battery dimension can be performed for a given panel size. This restricts the search process in one-dimensional space rather than in two-dimension; only one variable changes, the other remains constant. Therefore, for a given panel size $n_{PV} = n_{PV_0}$, the optimal number of battery units can be obtained from the following optimization problem:

$$\begin{aligned} \text{(P2)}: \underset{N_B}{\text{minimize}} \quad & C_B \cdot \frac{Y}{L(n_{PV_0}, N_B)} \cdot N_B + C_{PV} \cdot n_{PV_0} + \\ & A_{PV} \cdot n_{PV_0} \cdot Y \cdot C_R + C_{all} \\ \text{subject to:} \quad & P_{out}(n_{PV_0}, N_B) \leq p, \\ & -N_B \leq -N_{B_{th}}. \end{aligned}$$

It is important to characterize the optimization problem (P2) in order to find the optimal solution efficiently, as the nature of optimization problem will provide the clue to reach the optimal solution in a lesser time.

Lemma 1. *The total expenditure $C_{Ex}(n_{PV}, N_B)$ is a quasiconvex function of number of battery units N_B for a given panel size.*

Proof: See Appendix C. □

Lemma 2. *The outage probability $P_{out}(n_{PV}, N_B)$ is a convex function of number of battery units N_B for a given panel size.*

Proof: See Appendix D. □

Lemma 1 and Lemma 2 assure that (P2) is also a convex optimization problem, as the objective function is quasiconvex function of N_B and the constraints are convex function of N_B. Hence the optimal number of battery obtained from (P2) is global optimal for a given panel size, and there is no need to search for all values of N_B.

Remark 5. *For a given panel size, an optimal number of battery units obtained while satisfying the energy outage constraint is also global optimal due to convex nature of the optimization framework.*

Computationally-efficient Energy outage aware Cost-optimal Dimensioning Algorithm (CECoDA) is proposed in Algorithm 1 by taking advantage of convexity of the optimization problems (P1) and (P2). If energy outage constraint is not satisfied, then the total expenditure, which includes computation of battery life, is not calculated in order to save time. The optimal selection process starts from the lower bound of panel size $n_{PV_{LB}}$. Then the optimal number of battery units is estimated while satisfying the energy outage probability for this given panel size. The search stops when increase in cost function is noticed due to convex nature of (P2) (cf. Remark 5). Then, the panel size is increased by $\bigtriangledown n_{PV}$ and the optimal number of battery units is obtained. The cost of optimal combination with present panel size is compared with that of the previous panel size, and this process is repeated till the decrease in cost is noticed. This procedure yields optimum result due to convex nature of problem (P1) (cf. Remark 4). The search process stops due to convexity of (P1) and (P2), which ensure a global optimal solution. $\bigtriangledown n_{PV}$ is the incremental value of the PV panel size; $\bigtriangledown n_{PV}$ = 1 KW is considered in this work.

Algorithm 1 Computationally-efficient Energy outage aware Cost-optimal Dimensioning Algorithm (CECoDA)

1: **Required :** energy harvesting data, traffic profile, $\eta_c, \eta_d, p, C_{PV}, C_B, C_R, A_{PV}, \bigtriangledown n_{PV}$
2: **Ensured :** $(n_{PV}^{opt}, N_B^{opt})$
3: start with $n_{PV} = n_{PV_{LB}}$
4: start with $N_B = N_{B_{th}}$
5: calculate $P_{out}(n_{PV}, N_B)$ for given n_{PV} and N_B
6: **if** $P_{out}(n_{PV}, N_B) \leq p$ **then**
7: | compute $C_{Ex}(n_{PV}, N_B)$
8: **else**
9: | break
10: **end if**
11: **if** $C_{Ex}(n_{PV}, N_B) < C_{Ex}(n_{PV}, N_B - 1)$ **then**
12: | $N_B = N_B + 1$
13: **else**
14: | break
15: **end if**
16: $\mathfrak{N}(n_{PV}) = N_B - 1$
17: **if** $C_{Ex}(n_{PV}, \mathfrak{N}(n_{PV})) < C_{Ex}(n_{PV} - \bigtriangledown n_{PV}, \mathfrak{N}(n_{PV} - \bigtriangledown n_{PV}))$ **then**
18: | $n_{PV} = n_{PV} + \bigtriangledown n_{PV}$
19: | **goto** *step 4*
20: **else**
21: | stop
22: **end if**
23: Cost optimal system dimension: $n_{PV}^{opt} = n_{PV} - \bigtriangledown n_{PV}$ and $N_B^{opt} = \mathfrak{N}(n_{PV}^{opt})$
24: Optimal cost: $C_{Ex}^{opt} = C_{Ex}(n_{PV}^{opt}, N_B^{opt})$

7 Results and Discussion

Four cities New Delhi, Las Vegas, and Kansas located at different geographical locations as well as having diverse solar potential are considered for presenting validation results of the proposed framework. NREL data for several other cities, namely, Ahmedabad, Itanagar, Kolkata, Jaipur, Texas, Denver, Missouri, Illinois, Indiana, New York, have also been used for extensive testing and validation purpose. For brevity of presentation, the results on these cities are not included here. The values of battery efficiency parameters are $\eta_c = 0.9$ and $\eta_d = 0.9$. The power model for macro SS-BS is given in (2). The equation parameters are listed in Table 3 and traffic profile is shown in Fig. 2. Flooded lead acid battery with 12 V, 205 Ah capacity having depth-of-discharge $\delta = 0.7$ is considered. The cost of 1 KW rating PV panel is $C_{PV} = \$1000$; the cost of one battery is $C_B = \$280$. The time duration for long-run operation is considered as $Y = 10$ years.

7.1 Validation of Lower Bounds

The lower bound on PV panel size for different cities are obtained as: $n_{PV_{LB}} = 6$ KW for New Delhi, 8 KW for Itanagar, 5 KW for Las Vegas, and 7 KW for Kansas. The variation of energy outage probability for four different PV panel sizes in the neighborhood of lower bound, i.e., $n_{PV} = n_{PV_{LB}} - 1, n_{PV_{LB}}, n_{PV_{LB}} + 1$, and $n_{PV_{LB}} + 2$ against the number of battery units for the four cities are shown in Fig. 5. The panel size $n_{PV} = n_{PV_{LB}} - 1$ is not able to harvest sufficient energy required by load and frequent energy outage occurs due to this. The energy outage probability saturates for $n_{PV} = n_{PV_{LB}} - 1$ and no improvement in energy outage is observed even for higher number of battery

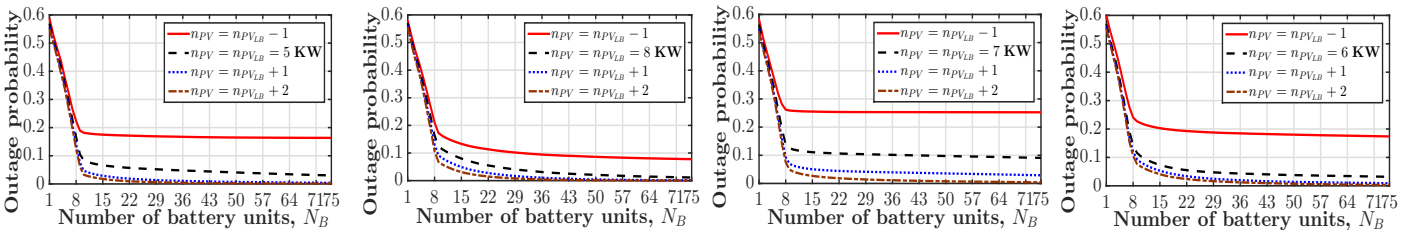

(a) New Delhi (b) Itanagar (c) Las Vegas (d) Kansas

Figure 5: Variation of energy outage probability versus number of battery units, with three panel sizes $n_{PV_{LB}} - 1, n_{PV_{LB}}, n_{PV_{LB}} + 1$, and $n_{PV_{LB}} + 2$ for four different cities.

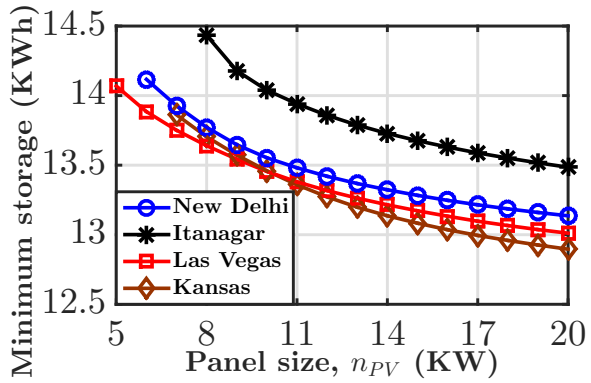

Figure 6: Lower bound on storage capacity for four different cities.

units due to lack of sufficient energy harvested. On the other hand, for the system with PV panel size $n_{PV_{LB}}$, $n_{PV_{LB}} + 1$, and $n_{PV_{LB}} + 2$, the energy outage probability tends towards acceptable range ($\leq 1\% = 0.01$) [4], [39] and even becomes zero at higher value of N_B. Significant improvement in energy outage probability is observed with increase in storage capacity as PV panel size increases, because the energy generated is stored in the battery, which is not possible when $n_{PV} = n_{PV_{LB}} - 1$. Here, for validating the bounds, simulation up to 75 batteries (approximately 185 KWh energy storage) are shown. In spite of such huge storage, the energy outage probability is far from acceptable range for system with $n_{PV} < n_{PV_{LB}}$.

The lower bound on storage capacity against the number of PV panels ($n_{PV} \geq n_{PV_{LB}}$) is plotted in Fig. 6 for the four cities. It can be observed that, as the PV panel size increases, the lower bound on storage capacity decreases. If the storage is divided in two parts: one in presence of solar radiation (day hours) and other in absence of solar radiation (night hours). The required storage decreases during day hours with increase in panel size, whereas no effect on storage is observed during night hours. It can be noted that, the minimum storage required for all four cities tend towards the same value with increase in the number of PV panels, and the difference is much less at $n_{PV} = 20$ KW compared to the capacity of a battery unit (approximately 2.46 KWh). This realizes the existence of $N_{B_{th}}$, and $N_{B_{th}} = 8$ for all the cities.

The variation of energy outage probability with four different number of battery units in the neighborhood of lower bound, i.e., $N_B = N_{B_{LB}} - 1, N_{B_{LB}}$, $N_{B_{LB}} + 1$, and $N_{B_{LB}} + 2$ against the number of PV panels for the four cities are shown in Fig. 7. It can be observed that, for $N_B = N_{B_{LB}} - 1$, the energy outage probability is very high and faraway from acceptable range, whereas for $N_B = N_{B_{LB}}$ it tends towards acceptable range. System dimension with $N_{B_{LB}} + 1$ and $N_{B_{LB}} + 2$, outage lies in acceptable range and even nearly zero for higher n_{PV}. The energy outage probability improves significantly as PV panel size increases and saturates at higher PV panel size due to lack of storage capacity. The simulations are shown up to 20 KW PV panel size, which is well sufficient from practical SS-BS deployment.

Based on the above discussion, it is deduced that for *green sustainable system*, the system dimension must satisfy $(n_{PV}, N_B) \geq (n_{PV_{LB}}, N_{B_{LB}})$. It is also observed that, very high energy storage is required for smaller PV panel size with acceptable energy outage and vice-versa. But, such type of system dimension will be very costly, which demands for cost-optimal system dimension estimation.

Remark 6. *If the PV panel size is less than its lower bound, i.e. $n_{PV} < n_{PV_{LB}}$, energy outage is faraway from acceptable range in spite of very large storage deployment.*

Remark 7. *If the number of battery units is less than its lower bound, i.e. $N_B < N_{B_{LB}}$, energy outage is faraway from acceptable range in spite of very large PV panel deployment.*

7.2 Accuracy of Cost-optimal System Dimensioning

The cost-optimal system dimension using the proposed CECoDA is obtained for three different energy outage probability constraints: $p = 1\%, 0.1\%$, and 0.01%; and the dimension estimates are compared with those offered by three different competitive dimensioning methods: CapEx-OpEx-ImpEx optimal dimensioning [15], [16], CapEx optimal dimensioning [19], and dimensioning based on days of autonomy criteria [23]. In Table 6, the estimated system dimension with these competitive methods are listed, with $C_R = 0$, i.e., the effect of implementation expenditure is not considered. It is noted that, CECoDA estimates the system dimension very accurately, and the optimal system dimension matches closely with that in [15], [16]. The cost of optimal system dimension using the methods reported in [19] and [23] is much higher compared to that offered by CECoDA. This indicates that, system dimensioning based on CapEx-optimality and that with days of autonomy criteria are not good choices for long-run operation of SS-BS. The impact of site rent on optimal system dimension is listed in Table 7 with $C_R = \$10$ and $A_{PV} = 5\ m^2$. In this scenario also, the approaches in [19] and [23] lead to over-dimensioning of SS-BS. In case of non-zero rent cost, the optimal panel size is relatively lower than that with zero rent cost. It may be observed that, relatively larger system dimension is required to satisfy the stringent energy outage constraint in both the cases, i.e., with $C_R = \$0$ and with $C_R = \$10$. The cost-optimal system dimension also indicates that, the solar potential of New Delhi is higher than Itanagar, whereas the solar potential of Las Vegas

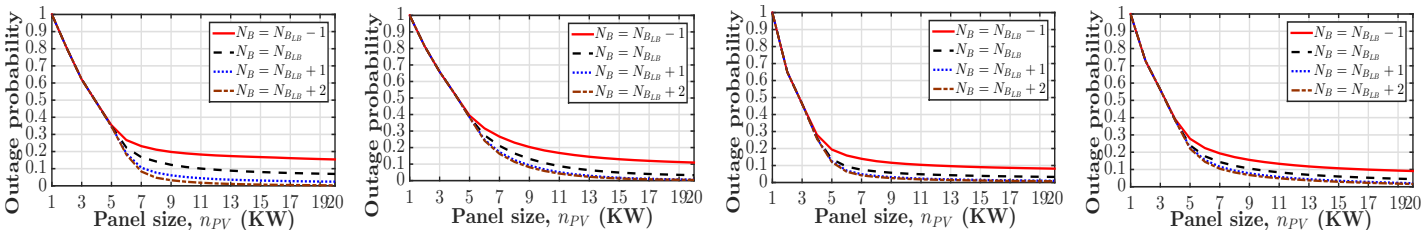

(a) New Delhi (b) Itanagar (c) Las Vegas (d) Kansas

Figure 7: Variation of energy outage probability versus PV panel size, with number of battery units $N_{B_{LB}} - 1, N_{B_{LB}}$, $N_{B_{LB}} + 1$, and $N_{B_{LB}} + 2$ for four different cities.

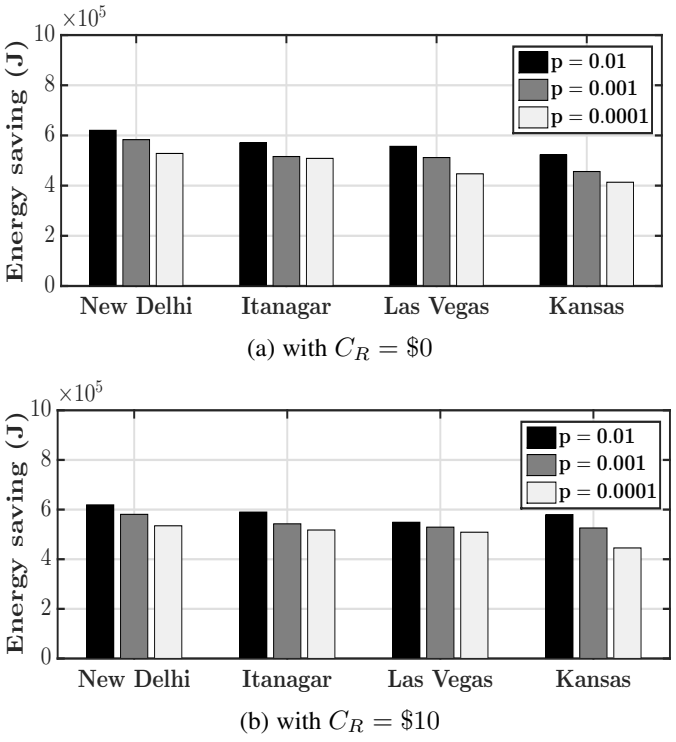

(a) with $C_R = \$0$

(b) with $C_R = \$10$

Figure 8: Saving in computation energy to find the cost-optimal system dimension in the $CECoDA$ over exhaustive search for four different cities having different energy outage constraint.

Table 6: Comparison of system dimension and cost estimates obtained by CECoDA with respect to the existing competitive methods, with $C_R = \$0$

	p	CECoDA	[15], [16]	[19]	[23]
New Delhi	1%	(9,15) $19,360	(9,15) $19,360	(9,21) $19,640	(12,17) $24,320
	0.1%	(10,29) $20,360	(10,29) $20,360	(11,22) $20,520	(13,28) $24,760
	0.01%	(13,32) $22,800	(13,32) $22,800	(15,19) $23,680	(15,35) $27,360
Itanagar	1%	(12,17) $23,200	(12,17) $23,200	(13,18) $23,360	(16,19) $28,320
	0.1%	(13,29) $23,640	(13,29) $23,640	(14,25) $24,080	(17,30) $29,040
	0.01%	(13,39) $24,480	(13,39) $24,480	(15,29) $25,080	(17,38) $29,600
Las Vegas	1%	(9,19) $19,920	(9,21) $19,920	(10,18) $20,360	(11,29) $27,240
	0.1%	(11,43) $23,320	(11,43) $23,320	(12,39) $23,760	(16,53) $31,960
	0.01%	(13,74) $29,520	(13,74) $29,520	(16,61) $30,280	(18,73) $36,480
Kansas	1%	(12,24) $24,600	(12,24) $24,600	(11,27) $ 24,720	(16,31) $35,320
	0.1%	(13,50) $28,120	(13,50) $28,120	(17,33) $28,480	(20,44) $36,800
	0.01%	(16,52) $30,040	(16,52) $30,040	(19,39) $30,760	(18,65) $39,000

is higher than Kansas. It requires to install relatively large PV panel and storage capacity to satisfy the same energy outage constraint for city having lesser solar potential, which incurs higher expenditure. Deployment of large PV panel and storage capacity overcome the lack of solar radiation by supplying more energy from PV panel and reserving more energy in the storage.

The discussion presented above reveals that optimal selection changes significantly with location, site rent, and energy outage constraint. This validates usefulness of the proposed framework. Total expenditure is minimum at the optimal solution, which is also the global minimum of expenditure; the search process stops here due to convex nature of the optimization problem.

7.3 Computation Efficiency of CECoDA

The cost-optimal system dimension estimation with the proposed CECoDA matches perfectly with the method used in [15], [16], where exhaustive search method is used. The time taken by CECoDA and that using exhaustive search [15], [16] to estimate the cost-optimal system dimension (cf. Table 6 and Table 7) are listed in Table 8 and Table 9 for $C_R = \$0$ and $C_R = \$10$, respectively. The simulation is carried out in Matlab 2015 software with Intel Core i7, 64-bit, 3.40 GHz processor having 16 GB random-access memory (RAM). The power consumption of the computer is 240 W. Significant saving in computation time up to 68%-94% by CECoDA is observed, which shows its importance in speeding up the dimensioning process. As the energy outage constraint becomes more stringent, time elapsed in computation increases due to requirement of relatively larger cost-optimal system dimension to satisfy the stringent energy outage constraint. The saving in computation time leads to huge amount of energy saving, which is shown in Fig. 8. Reduction in computation time or energy ranges in 68%-94%.

7.4 Cost Saving by using Modified Power Model

The cost saving, which is the difference of total cost of cost-optimal dimension from power model in (1) and the proposed

Table 7: Comparison of system dimension and cost estimates obtained by CECoDA with respect to the existing competitive methods, with $C_R = \$10$

	p	CECoDA	[15], [16]	[19]	[23]
New Delhi	1%	(8,20) $23,760	(8,20) $23,760	(9,21) $24,140	(11,21) $30,220
	0.1%	(10,29) $25,360	(10,29) $25,360	(11,22) $26,020	(13,28) $31,260
	0.01%	(11,49) $28,820	(11,49) $28,820	(14,43) $29,960	(16,28) $34,640
Itanagar	1%	(11,21) $28,820	(11,21) $28,820	(11,25) $29,100	(15,23) $36,220
	0.1%	(12,35) $30,040	(12,35) $30,040	(13,29) $30,640	(16,34) $37,160
	0.01%	(12,46) $30,380	(12,46) $30,380	(13,38) $30,980	(16,43) $38,000
Las Vegas	1%	(8,23) $24,040	(8,23) $24,040	(9,18) $24,140	(10,33) $33,200
	0.1%	(10,50) $28,720	(10,50) $28,720	(11,43) $28,820	(11,75) $38,060
	0.01%	(13,74) $36,020	(13,74) $36,020	(18,73) $37,120	(18,73) $45,480
Kansas	1%	(11,27) $30,220	(11,27) $30,220	(10,32) $30,400	(15,35) $43,780
	0.1%	(13,50) $34,620	(13,50) $34,620	(14,47) $35,280	(16,62) $47,240
	0.01%	(14,63) $37,520	(14,63) $37,520	(16,52) $38,640	(17,70) $48,180

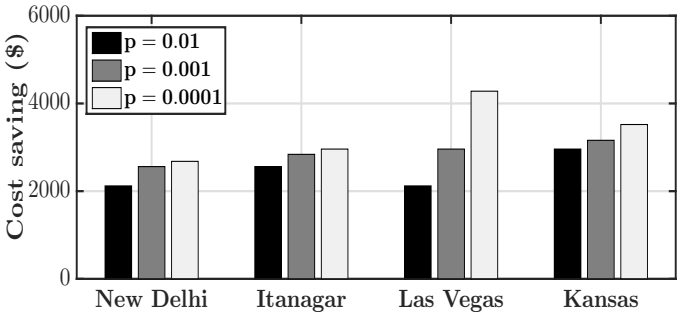

(a) with $C_R = \$0$

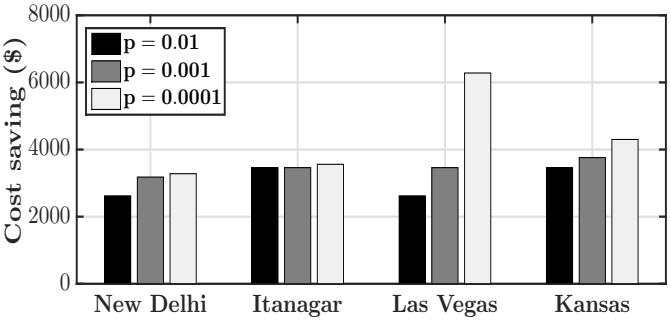

(b) with $C_R = \$10$

Figure 9: Cost saving for four different cities having different rent costs and different energy outage constraint.

modified power model for SS-BS in (2), is shown in Fig. 9 for four different cities and different energy outage constraints. The results indicate an appreciable saving of revenue by using the proposed power model. Cost saving ranges in 9%-15%, which becomes noteworthy in case of bulk deployment. This is because a smaller number panels and lesser number of battery units are required in case of modified power model to satisfy the same outage constraint.

7.5 Advantage of Proposed Framework

The amount of solar radiation reaching to the earth's surface varies greatly from location to location because of changing atmospheric conditions. Clouds are the predominant atmospheric condition, which determine the amount of solar radiation arriving to the earth surface. Local geographical features, such as mountains, oceans, and large lakes influence the formation of clouds [42]. Aerosols also lead to significant impairment on the solar radiation due to the scattering and absorption. Due to these reasons, even the places located nearby away may receive very different amount of solar energy. The dependency of solar radiation on several factors mentioned above do not allow to generalize the solar radiation profile. Instead, it is required to analyze the dimensioning procedure separately for each individual locations, which is computationally intensive. Towards this, the proposed framework will be useful, which overcomes the location dependency of solar profile from computation point of view while dimensioning. To investigate the location dependency of solar profile, we have selected two sets of locations from India; they belong to the same solar potential region classified by NREL. NREL has classified the regions of India by considering all the influencing factors mentioned above, and evolved a colored heat map, which indicates the solar potential of different regions [https://www.nrel.gov/]. The cities of the first set are Nashik, Pune, and Aurangabad, whereas Kargil, Leh, and Srinagar are the cities of the other set. The cities in each group are located nearby.

The lower bound on PV panel size for cities Nashik, Pune, and Aurangabad are 5 KW, 6 KW, and 6 KW, respectively; whereas the lower bound on PV panel size for cities Kargil, Leh, and Srinagar are 6 KW, 7 KW, and 8 KW, respectively. It is notable that, the lower bound for each set of cities are different, and cannot be generalized based on locality. This optimal system dimension for different energy outage constraint are listed in Table 10 for cities of each set. The cost-optimal system dimension is quite different for the cities of same set in spite of being in the same locality and same color zone of heat map. This observation reveals that, every location has its unique solar profile and needs separate analysis. In order words, the deployment of SS-BS with optimal system dimension obtained for dataset of a particular location will not satisfy the energy outage constraint with the same system dimension for the other nearby locations. This scenario leads to deteriorate the QoE perceived by the user as well as revenue model of operators due to over- or under-dimensioning. To this end, the proposed framework will play a key role by overcoming the location dependency of solar profile is system dimensioning, while sustainability reducing the computation overhead.

8 Conclusion

The power consumption model presented here for solar-enabled system is beneficial for green communication system design, which also saves significant revenue. In this proposed system characterization, the leftover energy has been modeled using Gaussian mixture model. Using this developed distribution, lower bounds on system dimension, i.e., PV panel size and number of battery units,

Table 8: Computation time (seconds) to find the cost-optimal system dimension using CECoDA and that using exhaustive search ([15], [16]), with $C_R = \$0$, along with percentage saving in computation time

	New Delhi		Itanagar		Las Vegas		Kansas	
	CECoDA	[15], [16]	CECoDA	[15], [16]	CECoDA	[15], [16]	CECoDA	[15], [16]
$p = 1\%$	191.69	2776.81	2657.14	281.64	256.14	2575.89	301.29	2477.10
	saving = 93.11 %		saving = 89.42 %		saving = 90.05 %		saving = 88.75 %	
$p = 0.1\%$	352.03	2782.32	2673.86	523.19	451.29	2584.67	588.30	2489.58
	saving = 87.34 %		saving = 80.43 %		saving = 82.54 %		saving =76.37 %	
$p = 0.01\%$	582.70	2783.41	2681.43	562.16	730.38	2593.21	779.87	2502.17
	saving = 79.05 %		saving = 78.97 %		saving = 71.84 %		saving =68.86 %	

Table 9: Computation time (seconds) to find the cost-optimal system dimension using CECoDA and that using exhaustive search ([15], [16]), with $C_R = \$10$, along with percentage saving in computation time

	New Delhi		Itanagar		Las Vegas		Kansas	
	CECoDA	[15], [16]	CECoDA	[15], [16]	CECoDA	[15], [16]	CECoDA	[15], [16]
$p = 1\%$	175.87	2754.23	175.87	2754.23	167.31	2583.17	381.02	2487.04
	saving = 93.61 %		saving = 92.25 %		saving = 93.53 %		saving = 84.68 %	
$p = 0.1\%$	347.87	2767.69	175.87	2754.23	405.73	2596.29	674.79	2504.61
	saving = 87.42 %		saving = 84.77 %		saving = 84.39 %		saving = 73.08 %	
$p = 0.01\%$	541.28	2769.11	175.87	2754.23	753.94	2609.09	798.53	2519.73
	saving = 80.42 %		saving = 80.13 %		saving = 79.13 %		saving = 68.32 %	

Table 10: Estimation of cost-optimal system dimension using CECoDA for two sets of cities of India for different energy outage constraint with C_R = \$0

	Nashik	Pune	Aurangabad	Leh	Kargil	Srinagar
$p = 1\%$	(9,16)	(9,18)	(9,14)	(10,19)	(11,20)	(14,20)
$p = 0.1\%$	(10,26)	(11,24)	(10,24)	(13,25)	(16,26)	(16,32)
$p = 0.01\%$	(10,37)	(12,32)	(11,32)	(14,35)	(19,38)	(19,42)

have been obtained, which determine the feasible search region for dimensioning. In the considered context of SS-BS, out of the total expenditure consisting of CapEx, OpEx, and ImpEx, OpEx depends on battery life, which has been obtained as a function of system dimension using curve fitting technique. The total cost has been proven to be a quasiconvex function, whereas energy outage has been proven to be convex function of system dimension. These properties transform the cost-optimal dimensioning problem into a convex optimization framework, which assures a global optimal solution. A computationally-efficient algorithm called CECoDA has been proposed to estimate the cost-optimal dimension while satisfying the given energy outage constraints without requiring exhaustive search. Four cities with widely varying solar irradiance, namely, New Delhi, Itanagar, Las Vegas, and Kansas, have been considered for numerical evaluation of the proposed dimensioning framework. Substantial saving in computation time and associated processing energy consumption along with excellent accuracy have been observed when applying proposed CECoDA as compared to the competitive exhaustive search based dimensioning. The computationally-efficient framework presented in this work will be very helpful to overcome the location-dependent unique solar profile while dimensioning.

REFERENCES

[1] K. Wang, X. Hu, H. Li, P. Li, D. Zeng, and S. Guo, "A survey on energy internet communications for sustainability," *IEEE Trans. Sustain. Comput.*, vol. 2, no. 3, pp. 231–254, July 2017.

[2] R. Antonello, M. Carraro, A. Costabeber, F. Tinazzi, and M. Zigliotto, "Energy-efficient autonomous solar water-pumping system for permanent-magnet synchronous motors," *IEEE Trans. Ind. Electron.*, vol. 64, no. 1, pp. 43–51, Jan. 2017.

[3] V. Pilloni, A. Floris, A. Meloni, and L. Atzori, "Smart home energy management including renewable sources: A qoe-driven approach," *IEEE Trans. Smart Grid*, vol. 9, no. 3, pp. 2006–2018, May 2018.

[4] V. Chamola and B. Sikdar, "Solar powered cellular base stations: current scenario, issues and proposed solutions," *IEEE Commun. Mag.*, vol. 54, no. 5, pp. 108–114, May 2016.

[5] H. Dou, Y. Qi, W. Wei, and H. Song, "Carbon-aware electricity cost minimization for sustainable data centers," *IEEE Trans. Sustain. Comput.*, vol. 2, no. 2, pp. 211–223, Apr. 2017.

[6] M. A. Marsan, G. Bucalo, A. D. Caro, M. Meo, and Y. Zhang, "Towards zero grid electricity networking: Powering BSs with renewable energy sources," in *Proc. IEEE Int. Conf. Commun. Wksp.*, Budapest, Hungary, June 2013, pp. 596–601.

[7] T. Ahmad, S. Kalyanaraman, F. Amjad, and L. Subramanian, "Solar vs diesel: Where to draw the line for cell towers?" in *Proc. ACM Int. Conf. Inf. Commun. Technol. Develop. (ICTD)*, May 2015, pp. 7:1–7:11.

[8] E. Ofry and A. Braunstein, "The loss of power supply probability as a technique for designing stand-alone solar electrical (photovoltaic) systems," *IEEE Trans. Power App. Syst.*, vol. PAS-102, no. 5, pp. 1171–1175, May 1983.

[9] G. B. Shrestha and L. Goel, "A study on optimal sizing of stand-alone photovoltaic stations," *IEEE Trans. Energy Convers.*, vol. 13, no. 4, pp. 373–378, Dec. 1998.

[10] C. V. T. Cabral, D. Oliveira Filho, A. S. A. C. Diniz, J. H. Martins, O. M. Toledo, and B. Lauro de Vilhena, "A stochastic method for stand-alone photovoltaic system sizing," *Sol. Energy*, vol. 84, no. 9, pp. 1628–1636, 2010.

[11] P. G. Nikhil and D. Subhakar, "Sizing and parametric analysis of a stand-alone photovoltaic power plant," *IEEE J. Photovoltaics*, vol. 3, no. 2, pp. 776–784, Apr. 2013.

[12] P. Arun, R. Banerjee, and S. Bandyopadhyay, "Optimum sizing of photovoltaic battery systems incorporating uncertainty through design space approach," *Sol. Energy*, vol. 83, no. 7, pp. 1013–1025, 2009.

[13] G. Leonardi, M. Meo, and M. A. Marsan, "Markovian models of solar power supply for a LTE macro BS," in *Proc. IEEE Int. Conf. Commun.*, Kualalumpur, Malaysia, May 2016, pp. 1–7.

[14] D. Renga and M. Meo, "Dimensioning renewable energy systems to

power mobile networks," *IEEE Trans. Green Commun. Netw.*, pp. 1–1, 2019.

[15] V. Chamola and B. Sikdar, "Power outage estimation and resource dimensioning for solar powered cellular base stations," *IEEE Trans. Commun.*, vol. 64, no. 12, pp. 5278–5289, Dec. 2016.

[16] S. Suman and S. De, "Solar-enabled green base stations: cost versus utility," in *Proc. IEEE WoWMoM*, Macau, China, June 2017, pp. 1–9.

[17] I. Abouzahr and R. Ramakumar, "Loss of power supply probability of stand-alone photovoltaic systems: a closed form solution approach," *IEEE Trans. Energy Convers.*, vol. 6, no. 1, pp. 1–11, Mar. 1991.

[18] L. Barra, S. Catalanotti, F. Fontana, and F. Lavorante, "An analytical method to determine the optimal size of a photovoltaic plant," *Sol. Energy*, vol. 33, no. 6, pp. 509–514, 1984.

[19] P. G. Nikhil and D. Subhakar, "Approaches for developing a regression model for sizing a stand-alone photovoltaic system," *IEEE J. Photovoltaics*, vol. 5, no. 1, pp. 250–257, Jan 2015.

[20] M. Sidrach-de Cardona and L. M. Lopez, "A simple model for sizing stand-alone photovoltaic systems," *Sol. Energy Mater. Sol. Cells*, vol. 55, no. 3, pp. 199–214, 1998.

[21] A. P. C. da Silva, D. Renga, M. Meo, and M. A. Marsan, "The impact of quantization on the design of solar power systems for cellular base stations," *IEEE Trans. Green Commun. Netw.*, vol. 2, no. 1, pp. 260–274, Mar. 2018.

[22] H. A. M. Maghraby, M. H. Shwehdi, and G. K. Al-Bassam, "Probabilistic assessment of photovoltaic (PV) generation systems," *IEEE Trans. Power Syst.*, vol. 17, no. 1, pp. 205–208, Feb 2002.

[23] N. Kakimoto, S. Matsumura, K. Kobayashi, and M. Shoji, "Two-state Markov model of solar radiation and consideration on storage size," *IEEE Trans. Sustain. Energy*, vol. 5, no. 1, pp. 171–181, Jan. 2014.

[24] R. S. Weissbach and J. R. King, "Estimating energy costs using a Markov model for a midwest off-grid residence," in *Proc. IEEE Green Technologies Conf.*, Denver, USA, Apr. 2013, pp. 430–434.

[25] A. Mellit, "ANN-based GA for generating the sizing curve of stand-alone photovoltaic systems," *Advances in Engineering Software*, vol. 41, no. 5, pp. 687–693, 2010.

[26] J. Song, V. Krishnamurthy, A. Kwasinski, and R. Sharma, "Development of a Markov-chain-based energy storage model for power supply availability assessment of photovoltaic generation plants," *IEEE Trans. Sustain. Energy*, vol. 4, no. 2, pp. 491–500, Apr. 2013.

[27] H. Wang, H. Li, C. Tang, L. Ye, X. Chen, H. Tang, and S. Ci, "Modeling, metrics, and optimal design for solar energy-powered base station system," *EURASIP J. Wireless Commun. Netw.*, no. 1, pp. 1–17, Feb. 2015.

[28] C. You, K. Huang, H. Chae, and B. Kim, "Energy-efficient resource allocation for mobile-edge computation offloading," *IEEE Trans. Wireless Commun.*, vol. 16, no. 3, pp. 1397–1411, Mar. 2017.

[29] System Advisor Model (SAM). National Renewable Energy Laboratory.

[30] G. Auer, V. Giannini, C. Desset, I. Godor, P. Skillermark, M. Olsson, M. A. Imran, D. Sabella, M. J. Gonzalez, O. Blume, and A. Fehske, "How much energy is needed to run a wireless network?" *IEEE Wireless Commun.*, vol. 18, no. 5, pp. 40–49, Oct. 2011.

[31] *Huawei Technologies Corporation Ltd. eLTE3.1 DBS3900 LTE FDD Product Description*, 2013, Issue 01.

[32] *Motorola Solutions Inc. RBS 6000 Series Base Station*, Product Spec Sheet, 2018.

[33] G. Piro, M. Miozzo, G. Forte, N. Baldo, L. A. Grieco, G. Boggia, and P. Dini, "Hetnets powered by renewable energy sources: Sustainable next-generation cellular networks," *IEEE Internet Comput.*, vol. 17, no. 1, pp. 32–39, Jan 2013.

[34] C. M. Bishop, *Pattern recognition and machine learning*. springer, 2006.

[35] R. B. D'Agostino, *Goodness-of-fit-techniques*. CRC press, 1986, vol. 68.

[36] S. D. Downing and D. Socie, "Simple rainflow counting algorithms," *Int. J. Fatigue*, vol. 4, no. 1, pp. 31–40, Jan. 1982.

[37] Trojan j185h-ac lead-acid battery data sheet. [Online]. Available: https://www.thesolarbiz.com/media/catalog/product/t/r/TrojanJ185H-ACDataSheets.pdf

[38] P. G. Guest, *Numerical methods of curve fitting*. Cambridge University Press, 2012.

[39] E. Marcus and H. Stern, *Blueprints for high availability*. John Wiley & Sons, 2003.

[40] K. Samdanis, P. Rost, A. Maeder, M. Meo, and C. Verikoukis, *Green Communications: Principles, Concepts and Practice*. John Wiley & Sons, 2015.

[41] S. Boyd and L. Vandenberghe, *Convex optimization*. Cambridge university press, 2004.

[42] M. Dunlap, G. Cook, B. Marion, C. Riordan, and D. Renne, "Shining On: A Primer on Solar Radiation Data," National Renewable Energy Lab. (NREL), Golden, CO (United States), Tech. Rep., 1992.

Suraj Suman received the B.Tech. degree in Electronics and Communication Engineering from Indian Institute of Information Technology, Design and Manufacturing Jabalpur, India, in 2013, and the M.Tech. degree from Indian Institute of Technology Patna, India, in 2015. He is currently pursuing the Ph.D. degree in the Department of Electrical Engineering at Indian Institute of Technology Delhi, New Delhi, India. His current research interests include green communications, energy harvesting, and aerial communication system.

Swades De [S'02-M'04-SM'14] received the B.Tech. degree in radiophysics and electronics from the University of Calcutta, Kolkata, India, in 1993, the M.Tech. degree in optoelectronics and optical communication from the Indian Institute of Technology Delhi, New Delhi, India, in 1998, and the Ph.D. degree in electrical engineering from the State University of New York at Buffalo, Buffalo, NY, USA, in 2004.

He is currently a Professor with the Department of Electrical Engineering, IIT Delhi. Before joining IIT Delhi in 2007, he was a tenure-track Assistant Professor with the Department of Electrical and Computer Engineering, New Jersey Institute of Technology, Newark, NJ, USA, from 2004 to 2007. He was an ERCIM Post-Doctoral Researcher with ISTI-CNR, Pisa, Italy, in 2004, and has nearly five years of industry experience in India on communications hardware and software development, from 1993 to 1997, and in 1999. His research interests are in communication networks, with emphasis on performance modeling and analysis.

Dr. De currently serves as a Senior Editor for the IEEE COMMUNICATIONS LETTERS, and an Associate Editor for the IEEE TRANSACTIONS ON VEHICULAR TECHNOLOGY, the IEEE WIRELESS COMMUNICATIONS LETTERS, the IEEE NETWORKING LETTERS, and the IETE Technical Review journal.

APPENDIX A
PROOF OF THEOREM 1

Proof: To investigate the nature of multivariate function, it is important to analyze the Hessian matrix of the given function. If the Hessian matrix is positive semidefinite matrix in the domain of definition ($n_{PV} \geq n_{PV_{LB}}, N_B \geq N_{B_{th}}$), then the function is convex function. If this condition is not satisfied then, the nature of eigenvalues of Hessian matrix are investigated.

The total expenditure is given as,

$$C_{Ex}(n_{PV}, N_B) = C_{CapEx}(n_{PV}, N_B) + C_{OpEx}(n_{PV}, N_B) + C_{ImpEx}(n_{PV}, N_B)$$

where $C_{CapEx}(n_{PV}, N_B)$, $C_{OpEx}(n_{PV}, N_B)$, and $C_{ImpEx}(n_{PV}, N_B)$ are provided in (13), (14), and (18), respectively.

The Hessian matrix of total expenditure is given as,

$$H_{Ex} = H_{CapEx} + H_{OpEx} + H_{ImpEx}$$

where H_{CapEx}, H_{OpEx}, and H_{ImpEx} are the Hessian matrix of $C_{CapEx}(n_{PV}, N_B)$, $C_{OpEx}(n_{PV}, N_B)$, and $C_{ImpEx}(n_{PV}, N_B)$, respectively.

The Hessian matrix of $C_{CapEx}(n_{PV}, N_B)$ is given by,

$$H_{CapEx} = \begin{bmatrix} 0 & 0 \\ 0 & 0 \end{bmatrix}.$$

Therefore, the $C_{CapEx}(n_{PV}, N_B)$ is a convex function of n_{PV} and N_B.

The Hessian matrix of $C_{OpEx}(n_{PV}, N_B)$ is given as,

$$H_{OpEx} = \begin{bmatrix} h_{11} & h_{12} \\ h_{21} & h_{22} \end{bmatrix}.$$

where h_{11}, h_{12}, and h_{21}, and h_{22} are given in (A.1), (A.2), (A.2), and (A.3), respectively.

The variation of determinant of H_{OpEx} for three different cities are shown in Fig. A.1. It can be noted that, $|H_{OpEx}|$ is not always positive over the domain of definition. Therefore, $C_{OpEx}(n_{PV}, N_B)$ is not a convex function of n_{PV} and N_B.

On the other hand, the Hessian matrix of $C_{ImpEx}(n_{PV}, N_B)$ is given as,

$$H_{ImpEx} = \begin{bmatrix} 0 & 0 \\ 0 & 0 \end{bmatrix}.$$

Therefore, $C_{ImpEx}(n_{PV}, N_B)$ is a convex function of n_{PV} and N_B.

Thus, the Hessian matrix of total expenditure is not positive semidefinite matrix in the domain of definition. Hence the cost function is not a convex function of n_{PV} and N_B. To characterize it further, it is important to investigate the nature of eigenvalues of the Hessian matrix. If the Hessian matrix has at most one negative eigenvalue, then it is said to be a quasiconvex function. The plots of maximum and minimum of two eigenvalues are shown in Fig. A.2 and Fig. A.3, respectively. One can observe that, one eigenvalue is always positive in the domain of definition, whereas the other is either negative or positive. This proves quasiconvex nature of the total cost as a function of n_{PV} and N_B.

□

APPENDIX B
PROOF OF THEOREM 2

Proof: The Hessian matrix of energy outage probability is given as,

$$H_{out} = \begin{bmatrix} \hbar_{11} & \hbar_{12} \\ \hbar_{21} & \hbar_{22} \end{bmatrix}.$$

where $\hbar_{11} = b_{10} \cdot e^{-n_{PV}} + b_{11} \cdot N_B \cdot e^{-n_{PV}} + 4 \cdot b_{20} \cdot e^{-2 \cdot n_{PV}}$, $\hbar_{12} = -b_{11} \cdot e^{-n_{PV}}$, $\hbar_{21} = -b_{11} \cdot e^{-n_{PV}}$, and $\hbar_{22} = 2 \cdot b_{02}$. The variation of determinant of H_{out} for three different cities are shown in Fig. A.4. One can deduce that, the Hessian matrix is positive definite and hence the energy outage probability is a convex function of n_{PV} and N_B.

□

APPENDIX C
PROOF OF LEMMA 1

Proof: The total expenditure for a given panel size $n_{PV} = n_{PV_0}$ is expressed as:

$$C_{Ex}(n_{PV}, N_B)\Big|_{n_{PV}=n_{PV_0}} = C_{PV} \cdot n_{PV_0} + C_B \cdot \frac{Y}{L(n_{PV_0}, N_B)} \cdot N_B + C_R \cdot n_{PV_0} \cdot A_{PV} \cdot Y + C_{all}.$$

To investigate the nature of single variable function, it is important to investigate the nature of second derivative. The second derivative of $C_{Ex}(n_{PV_0}, N_B)$ with respect to N_B is given in (C-1). The variation of $\frac{d^2 C_{Ex}(n_{PV_0}, N_B)}{dN_B^2}$ versus number of battery is shown in Fig. A.5 for different panel size in the domain of definition for different cities . The value of $\frac{d^2 C_{Ex}(n_{PV_0}, N_B)}{dN_B^2}$ is negative for some panel size. This indicates that, the $C_{Ex}(n_{PV_0}, N_B)$ is not a convex function of N_B.

Now, the first derivative of $C_{Ex}(n_{PV_0}, N_B)$ with respect to N_B is given as,

$$\frac{dC_{Ex}(n_{PV_0}, N_B)}{dN_B} = \frac{L(n_{PV_0}, N_B) - N_B \cdot L_{N_B}(n_{PV_0}, N_B)}{L^2(n_{PV_0}, N_B)}.$$

The variation of first derivative is shown in Fig. A.6 for different panel size and different cities. One can observe that, the first derivative changes sign only once for some panel size, whereas it does not change sign for some other panel sizes. This proves the quasiconvex nature of $C_{Ex}(n_{PV_0}, N_B)$ as a function of N_B for a given panel size n_{PV_0}.

□

APPENDIX D
PROOF OF LEMMA 2

Proof: The second derivative of $P_{out}(n_{PV_0}, N_B)$ is given as,

$$\frac{d^2 P_{out}(n_{PV_0}, N_B)}{dN_B^2} = 2 \cdot b_{02}.$$

One can observe from Table 5 that, $b_{02} > 0$ for all three cities, hence $P_{out}(n_{PV_0}, N_B)$ is a convex function of N_B. □

$$h_{11} = \frac{-L^2(n_{PV}, N_B) \cdot N_B \cdot L_{n_{PV}\ n_{PV}}(n_{PV}, N_B) + 2 \cdot N_B \cdot L(n_{PV}, N_B) \cdot L_{n_{PV}}(n_{PV}, N_B)}{L^4(n_{PV}, N_b)}$$

$$\text{with } L_{n_{PV}}(n_{PV}, N_B) = \frac{\partial L(n_{PV}, N_B)}{\partial n_{PV}} = a_{10} + a_{11} \cdot N_B + 2 \cdot a_{20} \cdot n_{PV} + 2 \cdot a_{21} \cdot n_{PV} \cdot N_B + a_{12} \cdot N_B^2 + 3 \cdot a_{30} \cdot n_{PV}^2,$$

$$L_{n_{PV}\ n_{PV}}(n_{PV}, N_B) = \frac{\partial^2}{\partial n_{PV}^2} L(n_{PV}, N_B) = 2 \cdot a_{20} + 2 \cdot a_{21} \cdot N_B + 6 \cdot a_{30} n_{PV}. \tag{A.1}$$

$$h_{12} = h_{21} = \frac{\begin{array}{r} -L^2(n_{PV}, N_B) \cdot \left[L_{n_{PV}}(n_{PV}, N_B) - N_B \cdot L_{n_{PV}\ N_B}(n_{PV}, N_B) \right] \\ + 2 \cdot N_B \cdot L_{n_{PV}}(n_{PV}, N_B) \cdot L(n_{PV}, N_B) \cdot L_{N_B}(n_{PV}, N_B) \end{array}}{L^4(n_{PV}, N_b)}, \tag{A.2}$$

$$\text{with } L_{n_{PV}\ N_B}(n_{PV}, N_B) = \frac{\partial^2}{\partial n_{pV}\ \partial N_B} L(n_{PV}, N_B) = a_{11} + 2 \cdot a_{21} \cdot n_{PV} + 2 \cdot a_{12} \cdot N_B.$$

$$h_{22} = \frac{\begin{array}{r} -L^2(n_{PV}, N_B) \cdot \left[L_{N_B}(n_{PV}, N_B) - N_B \cdot L_{N_B\ N_B}(n_{PV}, N_B) - L_{N_B}(n_{PV}, N_B) \right] - \left[L(n_{PV}, N_B) - \right. \\ \left. N_B \cdot L_{N_B}(n_{PV}, N_B) \right] \cdot 2 \cdot L(n_{PV}, N_B) \cdot L_{N_B}(n_{PV}, N_B) \end{array}}{L^4(n_{PV}, N_b)},$$

$$\text{with } L_{N_B}(n_{PV}, N_B) = \frac{\partial}{\partial N_B} L(n_{PV}, N_B) = a_{01} + a_{11} \cdot n_{PV} + 2 \cdot a_{02} \cdot N_B + a_{21} \cdot n_{PV}^2 + 2 \cdot a_{12} \cdot n_{PV} \cdot N_B + 3 \cdot a_{03} \cdot N_B^2,$$

$$L_{N_B\ N_B}(n_{PV}, N_B) = \frac{\partial^2}{\partial N_B^2} L(n_{PV}, N_B) = 2 \cdot a_{02} + 2 \cdot a_{12} \cdot n_{PV} + 6 \cdot a_{03} \cdot N_B. \tag{A.3}$$

$$\frac{d^2 C_{Ex}(n_{PV_0}, N_B)}{dN_B^2} = \frac{\begin{array}{r} -L^2(n_{PV_0}, N_B) \cdot \left[L_{N_B}(n_{PV_0}, N_B) - N_B \cdot L_{N_B\ N_B}(n_{PV_0}, N_B) - L_{N_B}(n_{PV_0}, N_B) \right] \\ - \left[L(n_{PV_0}, N_B) - N_B \cdot L_{N_B}(n_{PV_0}, N_B) \right] \cdot 2 \cdot L(n_{PV_0}, N_B) \cdot L_{N_B}(n_{PV_0}, N_B) \end{array}}{L^4(n_{PV_0}, N_B)}. \tag{C-1}$$

where $L_{N_B}(n_{PV_0}, N_B)$ and $L_{N_B\ N_B}(n_{PV_0}, N_B)$ can be obtained from (A.3) with $n_{PV} = n_{PV_0}$.

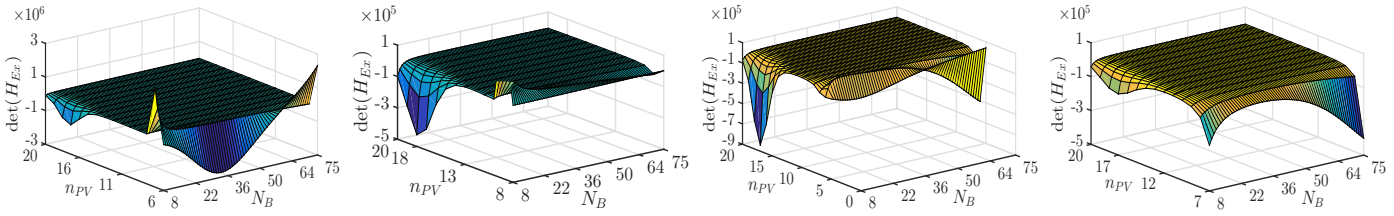

(a) New Delhi (b) Itanagar (c) Las Vegas (d) Kansas

Figure A.1: Variation of $|H_{OpEx}|$ versus panel size and number of battery units, for different cities.

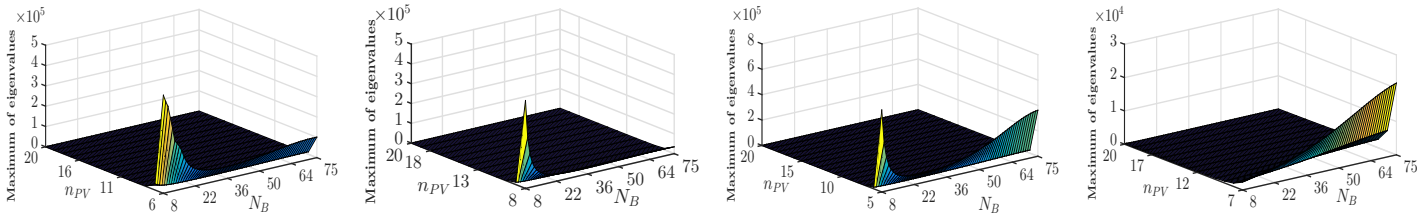

(a) New Delhi (b) Itanagar (c) Las Vegas (d) Kansas

Figure A.2: Variation of maximum of eigenvalues versus panel size and number of battery units, for different cities.

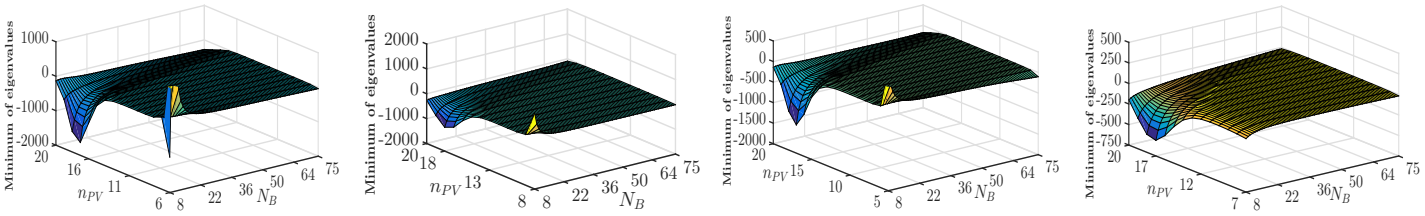

(a) New Delhi (b) Itanagar (c) Las Vegas (d) Kansas

Figure A.3: Variation of minimum of eigenvalues versus panel size and number of battery units, for different cities.

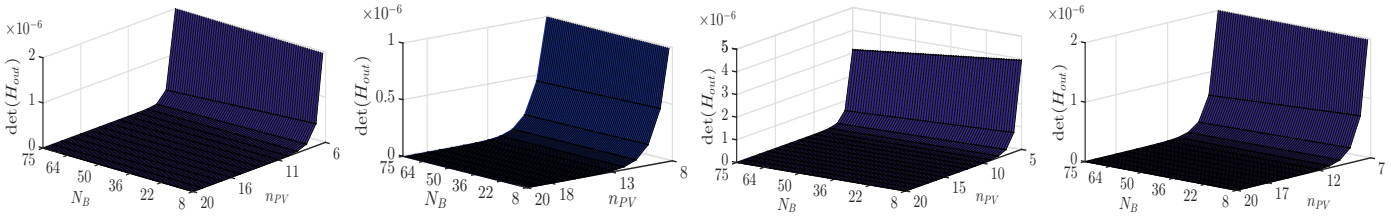

(a) New Delhi (b) Itanagar (c) Las Vegas (d) Kansas

Figure A.4: Variation of $|H_{Out}|$ versus panel size and number of battery units, for different cities.

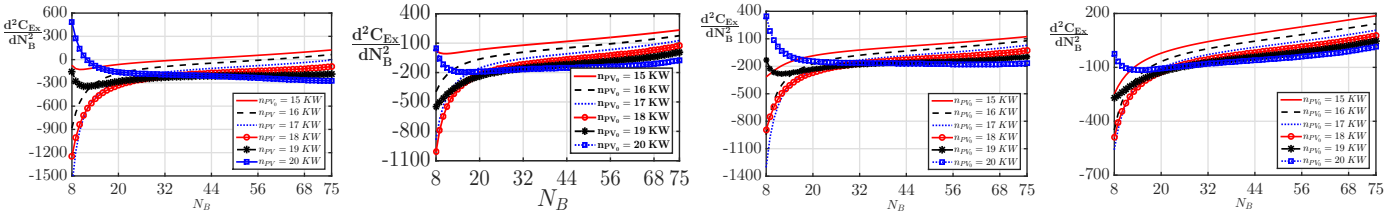

(a) New Delhi (b) Itanagar (c) Las Vegas (d) Kansas

Figure A.5: Variation of second derivative versus number of battery units for different panel size, for different cities.

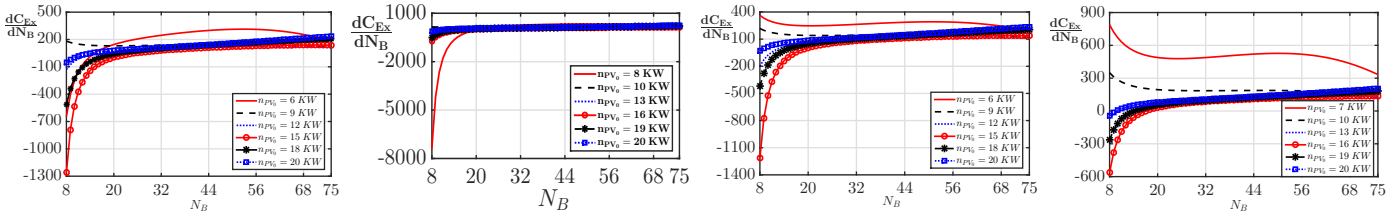

(a) New Delhi (b) Itanagar (c) Las Vegas (d) Kansas

Figure A.6: Variation of first derivative versus number of battery units for different panel size, for different cities.